LBL-21255

A Low Energy Cyclotron for Radiocarbon Dating

LBL--21255

DE86 009949

Ph. D. Thesis

James Joseph Welch

Lawrence Berkeley Laboratory
University of California
Berkeley, California 94720

December, 1984

This work was supported by the Dept. of Energy under Contract No. DE-AC03-76SF00098.

A Low Energy Cyclotron for Radiocarbon Dating

By
James Joseph Welch

Lawrence Berkeley Laboratory
University of California
Berkeley, California 94720

ABSTRACT

The measurement of naturally occurring radioisotopes whose half lives are less than a few hundred million years but more than a few years provides information about the temporal behavior of geologic and climatic processes, the temporal history of meteoritic bodies as well as the production mechanisms of these radioisotopes. A new extremely sensitive technique for measuring these radioisotopes at tandem Van de Graaff and cyclotron facilities has been very successful though the high cost and limited availability have been discouraging. We have built and tested a low energy cyclotron for radiocarbon dating similar in size to a conventional mass spectrometer. These tests clearly show that with the addition of a conventional ion source, the low energy cyclotron can perform the extremely high sensitivity 14C measurements that are now done at accelerator facilities. We found that no significant background is present when the cyclotron is tuned to accelerate 14C negative ions and the transmission efficiency is adequate to perform radiocarbon dating on milligram samples of carbon. The internal ion source used did not produce sufficient current to detect 14C directly at modern concentrations. We show how a conventional carbon negative ion source located outside the cyclotron magnet, would produce sufficient beam and provide for quick sampling to make radiocarbon dating milligram samples with a modest laboratory instrument feasible.

Introduction

Measurements of naturally occurring long lived radioisotopes provide information about the temporal behavoir of geologic and climatic processes, the temporal history of meteoritic bodies as well as the production mechanisms of radioisotopes in nature. We are mainly concerned here with long lived radioisotopes (LLRI) whose half-lives are more than a few years and less than a few hundred million years. Radioisotopes with half-lives less than a few hundred million years which were formed at the time of the formation of the elements over 5 billion years ago, have completely decayed by now. Consequently, if it were not for a few very weak production processes they would be entirely absent from natural materials. The isotopic abundance ratio of LLRI, (the ratio of the abundance of the radioisotope to the sum of the abundances of the stable isotopes of the same element), depends on the strength of the production mechanism, the absolute abundance of the stable isotope of the same element and the lifetime. The isotopic abundance ratio for most LLRI is usually on the order of 10^{-8} to 10^{-15}(1). Radioisotopes with halflives of a few years or less, such as ^{3}H (12 year half-life), decay so rapidly their isotopic abundance ratio can be well below 10^{-18}.

The primary production mechanism for most LLRI is through the action of cosmic rays on the upper atmosphere or on meteoritic material in space. Low Z radioisotopes such as ^{14}C (5700 year half-life) are primarily produced in the upper atmosphere where ^{14}N, ^{16}O, and ^{40}Ar are the target atoms. Higher Z radioisotopes are primarily formed in meteorites where heavier target materials are present. The natural radioactivity due to the presence of ^{238}U and ^{232}Th in minerals can also produce very small concentrations of radioisotopes which would otherwise be entirely absent. Recently, atmospheric

atomic bomb tests provided another major source of radioisotopes, although for a very short time. Among other things, these tests doubled the amount of ^{14}C in the atmosphere and increased the concentrations of ^{36}Cl (3×10^5 year half-life) per gram of sediment by about a factor of one hundred.

Measurements of concentrations of various LLRI per gram can often determine the origin of a material and provide clues about its history. Meteoritic bodies in space are exposed to the full intensity of the cosmic ray flux and develope concentrations of LLRI on the order of 10^4 times the concentrations in terrestrial surface materials which are shielded from the cosmic rays by the atmosphere. Some meteorites were once part of larger bodies which broke up. The outer layers of these bodies contain higher concentrations of LLRI, while the inner layers may contain concentrations of only those LLRI produced by neutron capture. Ice cores taken in Antartica show variations in the concentration of ^{10}Be per liter of ice which may be ascribable to variations in the intensity of the cosmic ray flux during the Maunder minimum. (1a)

Measurements of the isotopic abundance ratio of LLRI can provide precise knowledge about the absolute time history of a material. Radiocarbon dating is based on the determination of the length of time a sample has been removed from equilibrium with atmospheric CO_2 can be calculated by measuring the ratio of the abundance of ^{14}C to ^{12}C and comparing with the atmospheric value of 1.2×10^{-12}, which is known to have been approximately constant until the bomb tests. This technique might be extended to other radioisotopes with longer lifetimes such as ^{10}Be, ^{26}Al, and ^{36}Cl, provided one knows the initial isotopic ratio and the ratio does not change in such a way that there are many possible lifetimes for a given ratio. The half-lives of these radioisotopes are 1.6×10^6, 7.2×10^5, and 3.0×10^5 years respectively, and are

relevant to geologic and climatic processes.

Until recently, the measurement of the abundances of LLRI was performed almost exclusively by decay counting techniques. Decay counters can count as much as 50% of the decays of a sample and so in principle have very high efficiency. However, only a fraction of the radioisotope atoms in the sample will decay during the measurement period so the sensitivity to rare LLRI is severly limited by background and the amount of time a researcher is willing to wait. Clearly, for such radioisotopes a great enhancement of sensitivity is possible if the atoms are detected directly instead of detecting their decay.

Direct detection of ions of LLRI has been done since 1977 by employing cyclotrons and tandem Van de Graaff accelerators to ionize and accelerate sample atoms to high energy where individual radioisotope ions can be identified and separated from background ions using techniques of high energy physics (2). Though the overall detection efficiency of 10^{-4} to 10^{-5} is low compared to the detection efficiency of decay counters, the advantage of direct ion detection is so great that sample sizes in most cases can be reduced by a factor of 1000 or more. For example, conventional decay counting techniques require a few grams of carbon to measure the $^{14}C/^{12}C$ ratio, while the new method of direct ion detection by tandem Van de Graaff accelerators requires only a few milligrams. Furthermore, the ion sources used at these facilities are so powerful that the measurements can be made in about one hour or less - far less than decay counting times.

The process of cyclotron acceleration promises to be the key ingredient in the creation of a modest laboratory instrument to perform direct detection of LLRI. Sector focused, high energy cyclotrons, such as the 88" cyclotron at Berkeley, are capable of extremely good rejection of nonresonant masses as

well as high mass resolution (3). The large possible background of scattered ions of ^{12}C and ^{13}C from the source at the center of the cyclotron is completely eliminated by the acceleration process which systematically increases the energy of only ions with a narrowly defined charge to mass ratio. When the mass resolution is high enough, it is possible to identify different molecules and atoms on the basis of mass alone and to discriminate against all possible interfering molecules. We exploit these features at the energy of only 35 keV in order to greatly reduce the size of the magnet required and eliminate the need for any radiation shielding, and have constructed a cyclotron for ^{14}C measurements about the size of a conventional mass spectrometer (4).

The experiments presented here were aimed at determining the mass resolution and the background rejection possible with a low energy cyclotron. We show that the mass interference due to the molecule ^{13}CH, (which differs in mass from ^{14}C by 1 in 1800), can be eliminated by operation with many turns and a high harmonic number. We also argue that, in principle, the low energy cyclotron scheme could be developed for other LLRI or simply as an extremely sensitive mass spectrometer with only minor changes to the machine and a different ion source. We have not yet made an attempt to develop an ion source with sample changing capability, high intensity and high efficiency - these have been developed elsewhere and are used extensively at tandem Van De Graaff facilities. Finally, we show how a conventional ion source with full sample changing capabilities can be used to inject beam into the cyclotron where the acceleration will proceed as in the present system.

Applications

With the advent of direct detection of ^{14}C and the consequent reduction in sample size to the milligram level, the number and variety of samples which can now be measured has greatly increased and will continue to increase. New fields of study and new techniques in established fields have opened up which require $^{14}C/^{12}C$ measurements from large numbers of small samples in a relatively short time. Eventually, (it may already be true), the existing Tandem Van De Graaff facilities where these measurements can be carried out will be insufficient or too expensive to process all the samples (5). The availabilty, convenience, and small size of the low energy cyclotron, as it is conceived here, should allow researchers to obtain more systematic and thorough sampling using many new materials which had previously been too small to measure. For some applications the portability of a laboratory size instrument can substantially reduce sample collection and storage problems allowing immediate on site analysis.

The small size and portability of a low energy cyclotron for ^{14}C measurements would be a great advantage in the field of oceanography. A low energy cyclotron could put onboard a ship sent to collect seawater samples and sediment cores. ^{14}C measurements in seawater indicate the length of time deep currents have been out of ^{14}C equilibrium with surface waters where the ratio of $^{14}C/^{12}C$ is near the atmospheric value of 1.2×10^{-12}. When surface dwelling species of foraminifera die they quickily fall to the bottom where they are mixed with bottom dwelling species with older ^{14}C age (6). Paleocurrents can be studied by separating and dating the different types of forams taken from sediment cores. The forams must be separated by hand under a microscope so the sample size is extremely small and only direct detection methods for ^{14}C are feasible. Sample storage and collection problems would be

minimized since the analysis could be done immediately so more measurements could be made.

Another area where the availability and low cost of a low energy cyclotron would make it possible for more thorough and rapid measurements is the systematic study of ^{14}C concentrations in carbonaceous atmospheric gases. The ^{14}C concentrations in gases such as CO and CH_4 in the atmosphere could reveal sources and sinks of pollutents. For example, radiocarbon analysis of CH_4 might give a clue as to why CH_4 is increasing in the atmosphere at a rate of about 1% per year. Since these are trace gases (0.8 mg of CH_4/m^3 and .06 to 20 mg CO/m^3), it is imperative to be able to make measurements on very small amounts of carbon, otherwise the sample collection problem becomes enormous (7). Furthermore, it is desirable to collect and analyse many samples from different locations and at different times of the year to determine local and seasonal effects. One or more low energy cyclotrons could be dedicated to make these measurements so that samples could be processed quickily and inexpensively.

Finally, ^{14}C dating of archeological materials always involves a determination of authenticity and the amount of contamination by younger or older carbonaceous materials. Obtaining reliable dates is often very difficult even if there is adequate material for the ^{14}C measurement. The contamination problem can be solved by looking for consistency among dates from many subsamples of a larger sample, or among different samples found at the same location. It is desirable to date as many related pieces as possible to eliminate these uncertainties. Since the minimum sample size is only a few mg or less there is now a great variety of materials to date that can be found along with an artifact, such as pollen grains or seeds, some of which are reliable indicators of age. Altogether, there are a vast number of samples an

archeologist would find desirable to date and the low energy cyclotron would provide a means of obtaining these measurements quickily and economically.

II Design Requirements

Mass resolution and background rejection

High mass resolution and complete suppression of nonresonant masses are essential to the low energy cyclotron for the elimination of possible backgrounds at the level necessary for direct detection of ^{14}C and other long lived radioisotopes. High energy schemes for direct detection employed at tandem Van de Graaff and conventional cyclotron facilities unambiguously identify the accelerated ion by measuring the specific energy loss and the total energy deposited in ionization chambers or silicon detectors. The potential background of molecular ions $^{12}CH_2^-$ and $^{13}CH^-$ is greatly reduced since they are disintegrated at the stripping terminal of the tandem Van De Graaff accelerator (8). Neither of these techniques will work for ^{14}C at low energies (below 100 keV) because the ion velocity is too low for significant ionization to occur. Individual low energy ions can be detected efficiently by multiplying the secondary electrons emitted from an aluminum oxide surface when struck by an ion in an electron multiplier. However, low energy ion detectors cannot adequately distinguish between ^{14}C ions and other ions. Therefore all possible interfering ions must be suppressed before they reach the detector.

The main backgrounds which the low energy cyclotron must eliminate are the molecular ions of almost the same mass, $^{13}CH^-$ and $^{12}CH_2^-$, and ^{12}C and ^{13}C ions, which are extremely abundant compared to ^{14}C and might scatter to reach the detector. The potential background from ^{14}N is eliminated in the low energy cyclotron as it is in tandem accelerators by using negative ions, since nitrogen does not form stable negative ions. The next closest interfering molecule is then ^{13}CH, which differs in mass from ^{14}C by

1/1800. The mass 14 current from a standard carbon negative ion source is predominately composed of $^{13}CH^-$ and $^{12}CH_2^-$, and is expected to be 10^8 to 10^{11} stronger than the current of ^{14}C ions, depending on the age of the sample and the purity of the source material. The mass resolution of the cyclotron must therefore be sufficient to suppress the tail of the ^{13}CH current by a factor of 10^{-11}. Although the mass of ^{12}C is not very close to the ^{14}C mass, the current of ^{12}C is between 10^{12} and 10^{15} times the current of ^{14}C so one must be concerned about the extent of the suppression of ^{12}C and the possibility that some rather rare processes might allow ^{12}C ions to reach the detector, such as multiple scattering.

Conventional low energy mass spectrometer have not achieved the necessary transmission and suppression of interfering masses to measure ^{14}C directly. One attempt by Schnitzer and Anbar (9), using a strong negative ion beam on the order of 100 microamperes, ran into molecular interferences at the level of 10^{-7} of the source current. Through long and hard "chemical warfare" they were able to eliminate the source of many of the interfering ions and reduced the background to the 10^{-10} level before the effort was abandoned. Langeren and Stoffels (10) built a three stage mass spectrometer with 2 magnetic analyzers and one electrostatic analyser. They were able to achieve an abundance sensitivity at 1 amu mass separation of 2×10^9, without resorting to chemical warfare. However, the beam defining slits were only about .2 mm wide and the output currents were limited to only a few picoamperes - too small for radiocarbon dating.

The low energy cyclotron achieves the necessary background rejection through the cyclotron acceleration process and does not rely on elimination of interfering molecular ions from the ion source or source material. Furthermore, while conventional mass spectrometric methods obtain high mass

resolution by defining the momenta and positions of ions with slits and long trajectories, the low energy cyclotron uses the cyclotron frequency of ions in a uniform magnetic field which at low energies does not depend on momentum or position. As a consequence, the transmission efficiency in the low energy is much larger than it would be in a conventional mass spectrometer with the same mass resolution. Scattering of interfering ions by the residual gas to produce a background is not a problem in the low energy cyclotron despite its relatively modest vacuum of 2×10^{-7} Torr. Interfering ions never gain enough energy to be extracted or detected.

Current and Efficiency

The minimum useful ^{14}C count rate from the ion detector in the low energy cyclotron is determined by the background rate of the ion detector with no beam present, about 3 ct/hr. If the output current is not sufficient to provide that rate, very long counting times are needed to eliminate the uncertainty due to the background rate and the sensitivity of this method is reduced. We define the overall efficiency of the low energy cyclotron as the ratio of the number of ^{14}C ions detected to the number of ^{14}C atoms consumed by the ion source. The transmission efficiency is defined as the ratio of the rate ^{14}C ions are detected to the rate ^{14}C ions are produced by the source. In order to detect a minimum count rate of ^{14}C from a sample with the standard modern ratio of $^{14}C/^{12}C$ of 1.2×10^{-12} the product of the source current and the transmission efficiency must be at least 16.4 picoamperes. This product approximately represents the minimum output current the cyclotron should be capable of, neglecting possible space charge effects, when it is tuned to ^{12}C

rather than ^{14}C. If the sample is 30,000 years old, (almost 6 half lives), the product must be increased to 620 picoamperes.

The minimum overall efficiency required depends on the minimum sample size, maximum age, and minimum accuracy. A reasonable choice for these values for many applications involving small samples is 10mg, 30,000years, and 10% respectively. A 10% determination of the $^{14}C/^{12}C$ ratio of a 30,000 year old sample is an uncertainty of only 800 years or 3% in age. This choice yields a minimum overall efficiency of 6×10^{-6}, assuming the accuracy is statistics limited. Since conventional negative carbon ion sources convert about 8% of the sample carbon atoms to negative ions (11), the minimum transmission efficiency must be on the order of 10^{-3} to 10^{-4}.

Magnet size and radiation limit

The portability and modest size of the low energy cyclotron derive from the small size of the main magnet (30 cm pole diameter) necessary to confine the ^{14}C ions, and the fact that no radioactivity is produced. To contain a 35 kev ^{14}C ion requires only a 10kG magnetic field over a 20 cm diameter. Such fields can be produced by commercially available magnets weighing 1 to 2 metric tons. If Samarium cobalt permanent magnets were used the weight could be reduced to a few hundred kg. Similarly, the maximum energy that mass 12, charge 1, can reach in the low energy cyclotron at the extreme radius of the dees (12 cm) and the strongest magnetic field (13.8 kG) is only 110 keV. This is not sufficient to induce any radioactivity nor is there any x ray production by ^{12}C ions at such low energies. If hydrogen were accelerated

under the same conditions it would reach an energy of 1.3 Mev, enough to make a few low Z isotopes radioactive. High charge states of lighter isotopes could also obtain energies on the order of 1 MeV but would not be produced by the negative ion source nor would they induce more radioactivity than hydrogen. Only acceleration of dueterium could induce significant radioactivity if the beam strength were substantial. Consequently, no radiation shielding is needed provided one avoids loading the ion source with deuterium.

III Design

Overall

The path of a typical ^{14}C ion accelerated in the low energy cyclotron is shown in fig. 1a and 1b. Cesium ions formed near the center of a uniform 10 kG magnetic field are focused onto an axial strip (parallel to the magnetic field) on a carbon coated surface called the target. The cesium ion source is biased with only 100 volts which makes the orbit radius of the cesium ions about 1.7 cm. The target is biased at -2.8 kV and located behind a very fine grounded mesh. Negative carbon ions formed by the sputtering action of the cesium ions emerge with 2.8 keV energy and an orbit radius of 2.8 cm. They pass by the cesium source and enter the accelerating gap between the dees and the dummy dees. There they must gain at least 400 volts from the oscillating electric field in order to increase their energy and orbit radius to clear the grounded shielding around the carbon target on their first turn. If the ions are in resonance with the rf electric field, their energy increases to 35 keV and the orbit radius to 10 cm where they reach the deflector. The deflector consists of a thin grounded metal strip (the septum), parallel to an electrode at positive high voltage producing a strong radial electric field. When an ion enters the region between the septum and the electrode it is deflected out of the magnetic field toward a low background ion detector. There it stikes an aluminum oxide dynode at a glancing angle of 15 degrees and emits about 25 secondary electrons which are amplified by microchannel plate detector. The output of the microchannel plate detector is sent to a preamp and amplifier, and then to a discriminator/scaler.

Mass resolution

Harmonic acceleration, constant frequency and phase

For an ion to continually gain energy in the cyclotron, each time it crosses the accelerating gap between the dees and dummy dees, the direction of the electric field must be reversed from the previous crossing. While the ion is coasting deep inside the dees or in the grounded region behind the dummy dees the electric field may oscillate many times without affecting the ion. Consequentely the switching frequency of the electric field can be any odd multiple or "harmonic" of the revolution frequency and resonant acceleration will still occur. The revolution frequency or "cyclotron frequency" of an ion in a uniform magnetic field in cgs units is $f = qB/(2\pi mc)$, where q is the charge, B the magnetic field, m the mass and c the speed of light. The relativistic mass increase is insignificant in the low energy cyclotron, so to a very close approximation the frequency is independent of the energy. Therefore an ion with exactly the resonant mass will cross the gap at the same relative phase of the accelerating voltage waveform each revolution. This is a very important property since it allows ions at different energies to be simultaneously accelerated by the same periodic voltage waveform resulting in a relatively large output current.

Nonresonant Masses

Consider an ion with q/m different from a resonant value. If the mass is too light/heavy then the revolution frequency will be greater/less than the revolution frequency of the resonant mass and it will cross the gap at

successively earlier/later points in the voltage cycle. Eventually it will cross the gap when the electric field is in the wrong direction and start to lose energy. This process will continue until the ion has lost all of the energy it had gained and hits the ion source, or is lost for some other reason such as defocusing by the accelerating electric field. If the ion is not lost by the time it reaches the extraction radius, it will be removed from the cyclotron and detected.

The maximum energy a nonresonant ion can reach is calculated in a simplified case where the accelerating voltage waveform is sinusoidal, and the energy gain per turn is small compared to the energy and a smooth function of the number of turns (12). Then,

$$dE/dN = qV\cos\phi \tag{1}$$

where E is ion kinetic energy, N the number of turns, V the peak to peak amplitude of the rf voltage and, ϕ the relative phase of the rf cycle in which the ion passes the center of the gap (see fig 2). If ϕ_o is the starting phase of the ion then,

$$\phi = \phi_o + 2\pi NH\Delta f / f_o \tag{2}$$

where H is the harmonic number or ratio of rf frequency to cyclotron frequency, $\Delta f = f - f_o$, and f_o is the cyclotron frequency of the resonant mass. Substituting the expression for ϕ into equation 1 and integrating yields,

$$E = E_o + (qVf/\Delta f\, 2\pi H)\sin(\phi_o + 2\pi NH\Delta f/f_o) \tag{3}$$

where E_o is the initial ion energy. The energy is then an oscillating function of the number of turns. A more detailed analysis including some of the effects of the changing phase of the voltage while the ion crosses the gap is given in ref. (12).

The range in rf frequency in which a given ion can be accelerated is determined letting N vary and requiring the energy to reach the extraction energy. The resolution, $R = f_o/\Delta f$, is reduced if the ions start over a range of ϕ_o. There are however additional constraints on the phase that can increase the resolution. If the relative phase with which ion crosses the gap is very small or negative it will be lost due to lack of focusing or defocusing by the fringing components of the accelerating eletric field (discussed below). If the relative phase gets too large when the ion nears the extraction radius, the voltage gain per turn will not be enough for the ion to clear the septum (see fig. 2). If these limitations are put into equation 3 then one arrives at the mass resolution formula:

$$R = f_o/\Delta f = m/\Delta m \qquad (4)$$
$$= 2\pi H(E-E_o)/(qV(\sin\phi_{max} + \sin\phi_2 - \sin\phi_{min} - \sin\phi_1)).$$

The resolution R determines the full range in frequency for which there is an ion with an initial phase between ϕ_1 and ϕ_2 that can just reach the extraction energy E.

From the above expression it is clear that one can obtain high mass resolution by increasing Nres, or by increasing the harmonic number. Both ideas have been used successfully in the past. Very high mass resolution was obtained by L. Smith with his rf synchronometer which is essentially a two turn cyclotron operated near the 100th harmonic (13). Similarly, ion cyclotron

resonance devices (14), similar to the omegatron (15), used to study chemical reactions can resolve mass differences of 1 in 10^6 by allowing the ions to circulate thousands of times with no energy gain per turn. A burst of electrons from a filament is injected axially into the center of a uniform magnetic field to form ions from whatever gases are present in the device. This is followed by a burst of rf which starts the ions circulating. A periodic signal is obtained by measuring the induced current on nearby plates and the mass resolution is determined by the bandwidth which is limited by the time between collisions with residual gas atoms. Other schemes using cyclotron acceleration for mass spectrometry are reviewed in ref. (16).

Transit time effect

When the harmonic is high and the energy is low, the mass resolution is increased and the energy gained per crossing is considerably reduced from what is calculated above. This effect, called the transit time effect, occurs if the ion velocity is low enough that there is large change in the phase of the applied voltage during the time the ion is in the accelerating gap. If the harmonic is very high, the voltage may go through several complete oscillations before an ion can cross the gap region and enters the shielded region of the dees or dummy dees. As a result, the ion sees the average electric field which tends to zero and the energy gained per crossing is greatly reduced (see fig. 3).

In general, the strength of this effect depends on the shape of the electric field and the path an ion takes. Ions which cross the gap near the dee - dummy dee surface will gain more energy than those which pass through along the midplane, particularly if the gap is narrow, since they pass through the strong electric field region more quickly (see fig. 4). The transit time effect is

particularly strong during the early orbits and the ion velocity is low. The strength of the applied electric field must be increased for high harmonics to insure that ions gain enough energy on the first turn to clear the ion source. An analytic expression for the energy gain per gap crossing may be obtained in the approximation that there is zero gap between the dees and dummy dees by using either Fourier series or conformal mapping. The energy gain is proportional to a function of the form $V\cos(\phi)f(z,H/r)$ where z is the distance of the ion from the midplane between the top and bottom of the dees, and H/r where r is the orbit radius.

Resolving ^{13}CH

The transit time effect and especially the variation of the strength of the effect with the axial position of the ion, makes it difficult to analytically express the mass resolution. Equation 4, which ignores the transit time effect, was used to obtain a lower bound on the mass resolution to compute a first iteration design. In practice the rf voltage and harmonic number must be adjusted to achieve the necessary mass resoltuion.

Focusing

There are special difficulties focusing ions under the requirement of very high mass resolution. In conventional cyclotrons, ions are kept from drifting axially and striking the dees by the magnetic forces which are obtained by carefully shaping the magnetic field. In the original cyclotrons, the magnetic field strength was decreased slightly with increasing radius. The

cylinderical symmetry of the poles forces the existence of a small radial magnetic field whose sign changes above and below the midplane and acts as a restoring force to produce weak focusing. A shortcoming of this focusing method is that since the axial field is not quite uniform an ion which resonates at one radius will be nonresonant at all other radii. It turns out that this method can not be used in the low energy cyclotron because the energy spread from the ion source is large enough that, if the gradient in the magnetic field is kept small to allow constant frequency or "isochronous" acceleration, the focusing strength is far too weak and almost all the ions are lost. If the rf frequency is varied to match the changing magnetic field seen by the ions, ions can be accelerated only intermittently and much of the current from the dc ion source will be wasted giving a low overall efficiency.

Modern cyclotrons employ sector, or strong focusing. In the simplest case, the magnet for such a cyclotron consists of several pie shaped pieces arranged to give alternately thick and thin axial gaps producing variations in the axial magnetic field strength of up to 25%. Azimuthal variations in the axial magnetic field cause ions to move in noncircular orbits around the magnet. The interaction of the noncircular orbits and the radial components of the fringing field from the sectors produces a strong focusing force (17). To get enough focusing strength for use in the small cyclotron, the pie shaped pieces would have to be curved into spiral shapes to increase the radial field components. Maintaining exact isochronism necessary for high resolution, high transmission acceleration, necessitates measurements of the magnetic field, calculation of resulting orbits, and trimming the magnetic field to high accuracy. For these reasons an alternative scheme for focusing was sought and found - electrostatic focusing. Electrostatic focusing was found to be effective, convenient and practical.

Electrostatic focusing

The magnetic field used in the low energy cyclotron is kept as uniform as possible so virtually no magnetic focusing occurs and isochronism is relatively easy to maintain. Instead the ions are focused by the axial components of the electric field in the accelerating gap. When an ion crosses the accelerating gap the axial componenet of the electric field deflects it toward the midplane as it enters the gap and away from the midplane as it leaves. If the ion crosses the gap when the dee voltage is decreasing in time, the focusing deflection is larger than the defocusing deflection and there is a net focusing force (see fig. 5).

Beam blow up and biased ion source

Early papers by Rose (18) and Wilson (19) contain the essential ideas of electrostatic focusing as they pertain to conventional cyclotrons where magnetic focusing dominates. Their analysis shows that for all but the first orbit, the angle through which the ions off the midplane are deflected by the axial electric fields is proportional to $\Delta E/E$, where ΔE is now the energy gain per gap crossing. Axial momentum imparted by the electric field in the first few turns where $\Delta E/E$ is large, may be contained by magnetic focusing in later orbits. In the low energy cyclotron there is no magnetic focusing to compensate for the deflections given by the electric field during the first few turns. Consequentely, if the ions were extracted from the source directly by the dee voltage, the axial momentum would be much larger than could be contained by electrostatic focusing in subsequent orbits where $\Delta E/E$ is smaller

and the beam would rapidly diverge and hit the dees. This problem is almost eliminated if the ions are started with an initial energy that is substantially more than the energy gain per turn. We bias the ion source with about -3 kV while the energy gain on the first gap crossing is 400 to 700 volts. The problem is further reduced by the transit time effect which tends to increase the energy gained per gap crossing as the radius and energy get larger. For very high harmonics, above about 25, the focusing strength actually increases with radius. Orbits calculations discussed in the next section, which include the transit time effect show axial motion of the ions (see fig. 11a - 11d).

When ions are moving very slowly a different form of electrostatic focusing can occur because the ions travel through the defocusing region of the gap faster than through the focusing region. This effect is only significant when $\Delta E/E$ is of order unity. In the low energy cyclotron, with relatively large initial energy it is much less than the focusing due to phase change.

Ion source

The standard method for making negative carbon ions efficiently and with good emittance is to sputter a carbon surface with positive cesium ions. Carbon atoms can bind an electron to form a C^- ion with about 2.5 eV of binding energy. Cesium atoms effectively reduce the work function of the carbon surface so that it is energetically favourable for negative carbon ions to form. The sputtering process is needed to remove the carbon ion from the surface. Ionization efficiency, (ions formed/atom consumed), of almost 10% have been obtained. (11)

The complete ion source consisting of a cesium ion source and a biased carbon target is contained within the first 3 cm of the cyclotron (see fig. 1a).

The cesium source is manufactured by Spectra-Mat of Watsonville Ca., and is only 6mm in diameter and 2 cm long. A mixture of tungstun powder and cesium aluminum silicate, (essentially cesium ore) is sintered to form a stable button at the front of the ion source. Cesium atoms have an ionization potential of 1.3 eV while the work function of tungstun is around 4 to 5 eV. Thus it is energetically favorable for an electron to leave the cesium atom and go into the tungstun, leaving behind a cesium ion. The surface is heated to a maximum of 1100 degrees centigrade by a 10 watt noninductive heater wire and cesium ions evaporate from the surface with almost 100 percent efficiency. The current is limited by the rate at which cesium atoms/ions can diffuse to the surface. When the source is fresh and cesium atoms are near the surface the current density can be as high as 100 microamperes per cm^2. The usual operating current is on the order of 1 microampere per cm^2 - much smaller than conventional Cs sources. Cesium sources used at Tandem Van de Graaff facilities employ a reservoir of liquid cesium that is use to supply cesium vapour which diffuses through a porous tungstun surface. Since the diffusing cesium is replenished at a constant rate the current does not decline as it does in the source we used. Higher current densities are possible by increasing the temperature, without the problem of quickly expending all the available cesium. Furthermore, higher total currents are obtained, (on the order of 1 mA), since the area of the emitting surface can be made much larger than is possible in the very limited space available in the center region of the low energy cyclotron.

About 1 mm in front of the biased tungstun surface is a grounded copper mesh which pulls the ions from the source with 1 kV/cm electric field to give the cesium ions 100 eV. The radius of the cesium ion orbits is fixed at 1.7 cm. The beam curves through 90 degrees in the magnetic field and is radially

focussed onto the carbon target. The radial focusing is simply a result of the fact that in a uniform magnetic field the orbits are circular. Two circles of equal radii whose centers are displaced a small amount will intersect at a point 90 degrees from the line connecting the centers.

The design goal for the carbon target was to make the required first turn clearance as small as possible (see fig. 1a). This is critical since the transit time effect is most effective at reducing the energy gain on the first turn. If higher voltages are needed the number of turns must be reduced and so the resolution decreases. Carbon was vacuum deposited onto a thin molybdenum plate biased at -2.7 kV and located .75 mm behind a very fine grounded copper mesh. Cesium ions pass through the grid and hit the surface with 2.8 keV energy. The mesh and plate are kept as parallel and as close together as possible to obtain a very uniform accelerating field for the carbon ions. The width of the cesium beam spot on the target, at the 50% contour, is estimated (see below) to be 1.2 mm. If the center of the cesium beam is aimed 2 mm from the outer edge of the target, the electric field will be quite uniform over the entire beam spot and the first turn clearance is about 4 mm. The minimum energy gain on the first gap crossing is then about 400 eV. Because of the limited space available, a practical ion source with sample changing capability and far higher output current would be better located outside the magnet. Such sources are currently employed at tandem Van De Graaff facilities.

Extraction, detection, and normalization

Once the ions have reached the extraction energy and radius it is necessary remove them from the magnetic field and direct them to the ion detector. A 2 mm wide channel formed by two parallel electrodes contains a

uniform electric field (about 10 kV/cm) perpendicular to the magnetic field which forces ions away from the center of the magnet. The channel is curved in the opposite direction of the orbit curvature so the beam passes through the fringing field of the magnet quickly. The fringing field of the magnet axially focuses and radially defocuses the beam.

The extracted beam is directed through an opening in a magnetic shield to strike a highly polished aluminum oxide surface at an angle of 75 degrees to the normal to the surface. An average of about 25 electrons per incident carbon atom are emitted from the surface. These are accelerated into separate pores of a stacked microchannel plate detector to form a pulse an average of 25 times larger than a thermally generated single electron pulse (20). The detector has tested at using a well calibrated beam from a conventional mass spectrometer. It was demonstrated in the mass spectrometer that it is possible to set discriminator levels in to reduce the spontaneous detector background to less than 3 ct/hr and still count about 70 % of the carbon ions, though in the low energy cyclotron we only detect about 50%.

To obtain the ratio of $^{14}C/^{12}C$ or background rejection ratio the count rate must be normalized to the ion source output and the transmission efficiency. The background rejection ratio was measured by tuning the cyclotron to the ^{12}C mass and measuring the current at the detector position with a movable Faraday cup. Then the frequency was detuned and the Faraday cup replaced by the ion detector. An independent method was used to check the result. The ion source was turned down to very low power so the maximum output current could be put directly into the detector. Then the cyclotron was slightly detuned so the current dropped. The source power was then increased and the increase in count rate was recorded. This process was repeated several

times, each time moving the cyclotron tuning a little further from resonance so more total current could be used. Finally, when the source was at maximum power, the measured increases were multiplied together. The result agreed with the faraday cup measurement within a factor of 2.

IV Orbit Analysis

Introduction and definitions

Adequate transmission efficiency depends on a careful analysis of the emittance of the beam and the effects of various elements of the cyclotron. A complete analysis is complicated for two reasons. The first is that ions starting at different phases of the rf cycle see a different accelerating field and consequently follow completely different paths through the cyclotron. The second is that the focusing effects of the fringing fields of the dees are far from linear, especially at the higher harmonics, and the evolution of the orbits during acceleration can only be calculated numerically.

We define the transverse momentum P_t as the component of the momentum perpendicular to the average position of the beam. P_{tx} is the component of P_t in the plane of the cyclotron and P_{ty} is the componenet of P_t in the direction of the magnetic field (see fig. 6). E_t defined as $P_t^2/2M$, is the "transverse energy" and represents the kinetic energy associated with the motion of an ion about the fiducial trajectory. Initially, it is the intrinsic energy spread of the ions from the ionization process.

Initial emittance

Cesium emittance

We begin with the analysis of the cesium ion source since that determines the initial size of the carbon beam. Ultimately we are interested in the angular width of the beam and its size, i.e. the emittance. If we ignore the

presence of the biasing electric field for the present, then cesium ions evaporated from the source have a distribution in momenta and energies determined by the temperature of the tungstun surface. We assume the distribution is the same for ions as it would be for atoms at the same temperature and neglect the binding energy of the cesium ion to the surface of tungstun. Then the fraction of ions with energy $\mathcal{E}$ per unit energy is,

$$\rho(\varepsilon) = 2\beta\sqrt{\beta/\pi}\; e^{-\beta\varepsilon} \qquad (5)$$

where $1/\beta$ is Boltzmann constant times the temperature (21).

Under these assumptions, the angular spread of the beam is isotropic, but the focusing effects of the magnetic field make it convenient to derive the radial or axial angular spread separately. The fraction of ions with energy E and P_{tx} less than an arbitrary $/P_t/$ is, $(E_t/E)^{1/2}$ if E_t is less than E , and 1 if E_t is greater than E. Multiplying this expression with equation 5 and integrating over E yeilds the fraction of ions with P_{tx} less than an arbitrary P_t (see fig. 7a). The angular width of the beam about the beam path is:

$$\text{delta } \Theta = 2 \arctan(P_t/P) = 2 \arctan((E_t/E)^{1/2}) \qquad (6)$$

Equation 6 and the curve in figure 7a can be used to compute the fraction of the ion beam whose divergence in the horizontal plane is contained within a given angle. This together with the size of the source define the emittance of the cesium source and therefore the size of the cesium beam when it hits the carbon target.

Emittance growth from field defining meshes

Abberations from a uniform electric field caused by the finite size of the accelerating mesh can significantly increase the size of the cesium spot as well degrade the quality of the carbon ion beam formed. Since the transverse momentum an ion picks up passing through a mesh is not correlated to the transverse momentum it already had from the ionization process, the net transverse energy after passage through the mesh is on the average the sum of the initial transverse energy from the source and transverse energy picked up from the mesh.

We obtained an estimate for the size of this effect by finding an analytic expression for the electric field from a linear array of wires with line spacing a, at potential V with respect to a grounded plane, a distance b from the mesh where d is much greater than a. Trajectories were numerically computed using this expression and the increase in the transverse energy as a function of d/a and distance from the wire are plotted in figure 8a and 8b. The largest increase in tranverse energy is for ions which pass close to a wire where the rest of the wires have relatively little effect. An upper limit for the increase in E_t for a rectangular two dimensional mesh is made by equating the charge per unit length of wire in of the linear array with the charge per unit length of wire in the two dimensional mesh. Taking this into account as well as the focusing effects of magnetic field we estimate that approximately 50% of the cesium ions would strike within a spot 1 mm wide and about 3 mm high. Examination of figure 8a shows that given the choice of 79 wires/cm spacing, the additional transverse energy from passage of cesium ions through the mesh contributes a neglible amount to the width of the beam spot. If a 40 wires/cm mesh is used instead, the average increase in Et due to the mesh is comparable to the energy spread from the ion source.

Carbon emittance

The divergence of the negative carbon ion beam from the target is due to momentum transferred from the cesium ions when they strike the surface. An approximate phenomenalogical expression for the distribution of the energies of the secondary ions has been obtained by H. H. Anderson from computer model of the collision event (22). He found that if $n(\varepsilon)$ is the number of ions of energy ε (in eV) per unit energy,

$$n(\varepsilon) \sim \varepsilon/(\varepsilon + 2.5)^3 \qquad (7)$$

We assume the angular distribution of ions is approximately isotropic. Multiplying equation 7 by equation 6 and integrating as before we obtain the plot shown in figure 7b of the fraction of the carbon ions whose magnitude of horizontal momentum less than P_t, where $P_t = (2E_t/m)^{1/2}$. The effect of the finite number of wires in the biasing mesh on the carbon ions is illustrated in figure 8b.

Figure 9a shows the 62% contour of the radial emittance calculated for the carbon ion beam at the first gap crossing. The axial emittance at the source is essentially the same as the radial emittance except the beam fullwidth is an average of about 3 mm. The axial emittance at the first gap crossing is obtained by a simple mapping of the calculated source emittance through approximately 8 cm of drift space and shown in fig. 9b.

First Turn Clearance

The minimum distance to clear the ion source turns out to be the critical parameter limiting the transmission and ultimate mass resolution of the low energy cyclotron. It effectively limits the number of turns, the maximum feasible harmonic, the amount of rf phase available for acceleration, and the source emittance. To a good approximation the radial emittance of the beam after it has completed a full revolution and has to clear the source is the same as the radial emittance at the source because there is little change in energy and after 360 degrees of rotation the orbits close. We require that all of the ions within the 50% radial emittance contour must clear the ion source. In the low energy cyclotron, the fiducial path must move out 4 mm after one turn which implies a minimum $\Delta E/E$ per gap crossing of about 0.15. If the radial emittance were larger, the necessary first turn clearance would be greater, forcing $\Delta E/E$ to increase and the resolution to decrease. We note that a gas electron bombardment ion source could be designed which would allow passage of ions through the source on the first turn so $\Delta E/E$ could be quite small. Such sources may be feasible for other long lived radioisotopes besides ^{14}C. Axial or radial injection of ions from an external ion source into the center region would obviate some the difficulties in the first turn and are discussed in the final section.

Focusing

Ion trajectories through the dees were determined by computer calculations using an approximate analytic expression for the electric field in the gap. The analytic expression was arrived at by the methods of conformal

mapping assuming there is no gap between the dees and the dummy dees and is derived from the potentiál,

$$\delta(x,z) = V - (V/\pi)(\cos(\pi z/b)/\sinh(\pi x/b)) \tag{8}$$

where V is the peak dee voltage, z the distance of to the midplane between the top and bottom of the dees, and x is the distance to the midplane between the dees and the dummy dees. A gap of approximately .5 mm is needed to prevent breakdown across the gap, so the approximation does not give reliable results if the ion path comes within about .5 mm of the dee surface.

We found that at high harmonics the focusing force is much stronger when the ion passes close to the dee surface while at low harmonics the force is approximately linearly proportional to the distance from the midplane. (see fig. 10) The angular deflection may be expressed in the form:

$$\Delta\Theta = V/E \sin\phi\ g(z,H/r). \tag{9}$$

Betatron frequency

The axial betatron frequency V_z, is defined as the ratio of the axial oscillation frequency to the orbital frequency. For slow changes in V_z the amplitude of the axial oscillation is proportional to $1/V_z$. In conventional sector focused cyclotrons, considerable care is taken to keep the amplitude constant and avoid values of V_z close to comman rational fraction such as ½ or ¼ Axial oscillations can be resonantly excited by the perturbing effects of the magnetic field which the ion sees at harmonics and subharmonics of the cyclotron frequency (17). The orbital motion in the low energy cyclotron is not

disturbed by the large variations in the magnetic field used in sector focused machines; the only perturbing force is from the electric field in the dee gap whose axial components provide focusing. Futhermore, V_z in the low energy cyclotron ranges between 0.04 to 0.2 and is not constant over the entire trajectory of a given ion since the strength of the electrostatic focusing varies with rf phase and ion energy. A few examples of the computed ion axial trajectories are shown in figure 11a-11d.

Figure 11 shows that at high harmonics, the axial beam size first decreases and then increases with increasing radius, rather than the slow growth typical of electrostatic focusing. The rapid reduction of the strength of the transit time effect with increasing energy can for sufficiently high harmonic cause Δ E/E to increase with radius and is responsible for the convergence of the beam at the 31st harmonic shown in fig. 11d. Eventually the change in the transit time effect no longer compensates for the increasing energy and the beam diverges slowly.

Acceptance

Once the ions are clear of the source the axial focusing from the electric fields in the dee gap is able to contain 50% of the ions within the 62% contour of the axial emittance plot, at 4 degrees of rf phase. At 30 degrees, about 90% of the ions in figure 8b are accepted. The calculated maximum axial emittance at the extraction radius is shown in figure 12. The axial acceptance of 2700 keV ^{14}C ions is shown in figure 13.

Phase shift due to radial emittance

There is a complication in the analysis of the beam trajectories when a finite radial emittance is introduced. A resonant ion whose orbit center does not lie exactly on center of the dee gap will undergo a different angular rotation during the passage through the dees than in the dummy dees and consequently will not see the same rf phase on successive gap crossings. In general, such an ion will gain more energy from crossing on one side than the other and the orbit center will "walk" along the dee gap, thereby increasing the radial emittance. The difference in phase between successive gap crossings equals the harmonic times the radial emittance angle. For a radial emittance angle of 20 mrad and the 15th harmonic, the phase difference is 0.3 radians or 18 degrees. The worst case occurs when the relative rf phase is large and there is a large change in voltage for a given change in phase. At the large rf phase of 60 degrees there would be a 30% difference in the energy gain for the above mentioned ion between the two sides. By the time the ion reaches the extraction energy, this can cause the orbit center to drift almost 1 cm along the dee gap away from the early phase side . The consequence of a large spread in the centers of the ion orbits along the dee gap is to increase the range of energies of ions found emerging from the dee at a given radius, or to increase the spread in radial angle of ions found directly opposite the dees. This increase in the radial emittance of the beam can have important consequences for extraction efficiency.

Extraction

The deflector not only removes ions from the magnetic field but also

performs velocity selection and radial focusing of the beam. The range in energy that the deflector can accept can be approximately determined by plotting the trajectories with the corresponding minimum and maximum radii. The radial focusing force arises from the cycloidal motion of an ion in crossed electric and magnetic fields. The fact that the channel is curved has only a minor affect on the focusing properties. The calculated radial admittance of the deflector is shown for the low energy cyclotron in figure 14.

The radial emittance of the beam at the extraction energy neglecting the phase shift effect, is essentially the same at the initial radius except the angles are about 1/3 as large due to the higher energy. This means that if we ignore the phase shift effect there should be very little beam loss through the deflector. Most ions lost during extraction stike the leading edge or side of the septum, or have the wrong energy. Axial losses are not significant because of the shortness of the channel.

Detection

Immediately after ions emerge from the deflector they pass through the fringing field of the magnet at 30 degrees with respect to the radial direction and are axially focused and radially defocused. When the beam reaches the detector the calculated radial width is 7 mm and the axial width is about 5 mm. The beam stikes the aluminum oxide dynode at a glancing angle of 15 degrees from the surface. At this angle the dynode presents a 4.7 mm axial and 12.7 mm radial width so no significant beam is lost here provided the detector is in the proper position. The glancing angle is necessary to increase the number of secondary electrons which are emitted, allowing for higher discriminator levels and ultimately lower background rates.

V Performance

There are three criteria that the low energy cyclotron must meet to prove its usefulness: extremely good suppression of nonresonant masses, high mass resolution to completely suppress $^{13}CH^-$, and adequate transmission efficiency. The suppression of nonresonant masses is best demonstrated in figure 15. This curve shows the extent to which the tails of the main resonance drop off. When the frequency is off the peak by 1/1800, (the difference in mass between ^{14}C and ^{13}CH), the count rate has dropped to the detector background. This implies an abundance sensitivity of 2×10^{-11} at a mass difference of 1/1800 or 1/150 amu. The width of the peak could be reduced by decreasing the rf voltage or increasing the harmonic, however this would also result in a reduction of the peak height. This particular tuning was chosen because it gave the most current while maintaining essentially zero background at 1/1800 change in frequency. The tails of the tuning curve drops off on the high frequency side by a factor of 4×10^4 for a change in frequency of 1/14000. If the curve continues to fall off at this rate below the detector background then even a small increase in resolution would improve the rejection factor greatly.

Adequate mass resolution is demonstrated in figure 16 which shows the tuning curve near the ^{14}C resonance. Figure 16 clearly shows that ^{13}CH can be cleanly separated from ^{14}C. Complete separation of the entire tuning curves of ^{13}CH and ^{14}C is not necessary. The relavent separation distance is from the ^{13}CH peak to the point where ^{13}CH no longer produces a significant count rate. If the optimal tuning of ^{14}C lies to the right of that point then no significant background of ^{13}CH will be observed. No real ^{14}C counts were observed because the ion source did not produce sufficient current to observe

natural levels at a rate greater than the background from the ion detector.

Shape of tuning curve

The shape of the tuning curve is characteristically asymetrical with a steeper decline on the high frequency side (see fig. 15 and 16). This important feature can be explained as follows. When the rf frequency is above the resonant frequency ions migrate to larger rf phases (see fig 2) where they receive less and less energy gain per turn. Consequently more turns are required to reach the extraction energy than if they had been in exact resonance. A larger number of turns implies the net phase shift for a given frequency change is larger. If the rf frequency is below resonance ions migrate toward phases with higher accelerating voltages and need fewer turns to reach the extraction energy, thus they have a smaller net phase shift for given frequency change. If the phase gets below ϕ_{min} or above ϕ_{max} the ions will be lost, so the tuning is more sensitive on the high frequency side of the resonance.

By comparing the tuning curves for high rf voltage, where the resolution is less, and low rf voltages, where the peak must lie closer to the resonant frequency, it was found that peak count rate occurs slightly above the resonant frequency. As mentioned above, when the rf is above resonance ions migrate to larger rf phases where the focusing strength is greater, and this partly compensates for the decrease in overall focusing as $\Delta E/E$ gets smaller. One consequence of this is that the peak lies closer to the high frequency drop off. Since the ^{14}C resonance lies to the right of all molecular interferences (molecules are heavier) the required resolution is effectively reduced by almost 50%.

Width of Curve

Approximate values for the full width may be calculated from equation 4 provided one knows the maximum and minimum phase and the intial distribution of ions phases. The transit time effect makes the calculation more complicated by reducing the energy gain per turn different amounts depending of energy and axial position, but at low harmonics this should not be important. We estimate the effect of the transit time effect on mass resolution by increasing the resolution by the ratio of the number of turns ions execute on the computer simulation to the minimum number of turns with no transit time effect. When estimates for the intial phase distribution and minimum and maximum phase, based on the minimum clearance for the ion source and septum, are put into equation 4, it is found that the resolution is comparable to the predicted values but with considerable variations especially in the low resolution cases, where the scatter is considerable, (greater than 50%).

Transmission

An accurate measurement of the overall transmission efficiency has been difficult to obtain due to the relatively large amounts of mass 16, 13, and 24 currents from the ion source, which substantially increase the probe current close to the ion source. The relatively large initial current is a combination of carbon at the wrong phase, nonresonant masses, and ^{12}C ions which are not focussed sufficiently. A typical plot of current versus probe position is shown in figure 17. The decrease in current from 5 to 10 cm (which includes 3/4 of

the total number of turns) does not include the effects mentioned above. We find that in that interval, if the rf voltage is high there is a 40% loss of current, while if the voltage is low, and resolution high, there is a 70% loss.

The transmission through the deflector is about 50%. This loss is due to the rather thick septum, .025 cm, the fact that when the ions reach the deflector they have drifted in phase toward smaller turn spacing. The finite radial emittance of the ions at the extraction radius also contributes to the loss. Once the ions have passed through the deflector the efficiency of transmission is close to 100%. The dynode of the detector is slightly smaller than the calculated beam size but the main loss of efficiency at the detector, (about 50%), is due to the high discriminator level on pulse height that is necessary to reduce the background level of the detector.

Mulitiplying all of the above losses together and assuming 90% of the beam is lost near the source, yields an overall efficiency of ions detected divided by ions produced at the source of about 0.5% to 1%. If the cyclotron is tuned to mass 12 and if a 10 microampere beam is produced by the source, the current striking the detector should be 50 to 100 nanoamperes. If the cyclotron is tuned for ^{14}C then modern carbon would give a count rate of 0.5 to 1 count/sec. Our present source produces about 1 nanoampere of C^- beam rather than the 10 microamperes typical of conventional sources. We believe we can inject the beam from a conventional ion source into the center of the cyclotron.(see next section).

The ion source efficiency in the low energy cyclotron, (the ratio of the number of ^{14}C atoms detected to the number of ^{14}C atoms consumed), has not been determined. However, since the source is very similar in principle to sources with ionization efficiencies of around 10% a crude estimate is 10^{-3}. Therefore, 100 ^{14}C counts from 30,000 year old carbon could be obtained from

only about 0.1 mg of carbon.

VI Conclusion

Summary

We have shown that we are able to obtain sufficient mass resolution to cleanly separate ^{14}C and the closest possible interfering mass ^{13}CH. We have demonstrated that the the low energy cyclotron can measure abundance ratios of less than or equal to 2×10^{-11} at the mass separation of ^{13}CH and ^{14}C. Furthermore, we have argued that the ionization efficiency and transmission efficiency through the cyclotron to the detector is sufficient to date mg samples of 30,000 year old carbon to less than a 10% statistical uncertainty. We have not detected ^{14}C at natural levels because the maximum ion source current is insufficient to give a ^{14}C count rate above the detector background rate.

Prospects

We believe that the addition of an external conventional sputter type negative carbon ion source will overcome the previous limitation on source current as well as facilitate rapid sample changing necessary for practical instrument. Such sources typically produce a 10 microampere beam of ^{12}C as well as a beam of $^{12}CH_2$ and ^{13}CH of approximately 10^{-4} as much. The low energy cylotron should be able to suppress the background at the ^{14}C frequency form the ^{13}CH peak by a factor of 2×10^{-11} or better. Therefore the $^{14}C/^{12}C$ background can be measured at, or below, 2×10^{-15}. Furthermore, using the transmission efficiency of 0.5% to 1%, the ^{14}C count rate for modern levels would be about one count every 2 seconds. In comparison, a decay counting

instrument with 50% efficiency would detect 1 decay every three hours from a 1 mg sample of modern carbon.

The estimate of one count every 2 second assumes the emittance of the conventional ion sources is the same as the source used in the low energy cyclotron and there is no emittance growth due to space charge effects or optics. The sputtering process used in the present ion source is identical to that used in the conventional source except the cesium ion strikes the target with only 3 keV rather than the conventional 6 keV. The high energy tail of the sputtered carbon ions will extend further in a conventional source (see eq. 8) but will effect only a small fraction of the ions. In fact, the conventional source emittance of 2 - 3 π mm mrad $(\text{Mev})^{\frac{1}{2}}$ for 70% of the beam, is axially contained within the calculated axial acceptance of the low energy cyclotron down to about 4 degrees of rf phase for an ion energy of 5 keV (see fig. 12). The mass 12 and mass 13 currents will be separated before injection, and measured in Faraday cups. Space charge effects in the mass 14 injected beam are not expected to be significant with currents at the few nanoampere level. Furthermore, the mass 14 beam would be comparable in magnitude to the mass 12 beam we can obtain with the present ion source so space charge effects should not be greater than in the present experiment.

The main difficulty of an external source is injection of the beam. In conventional high energy cyclotrons axial injection is accomplished by sending the beam down a hole bored along the axis of the magnet yoke into 90 degrees electrostatic mirror which puts the beam into the plane of the cyclotron. This creates a nonuniformity in the magnetic field. We propose instead to inject the beam radially as shown in figure 18. The 5 keV mass 14 beam will be sent through a buncher which should be able to bunch at least a factor of ten given the energy spread of the ion source without substantially increasing the energy

spread of the beam. The beam is then radially focused onto the exit aperture of a narrow channel similar to the deflector, located just outside the last orbit radius. When it emerges from the channel, it executes a 180 degree turn before it hits an electrostatic mirror which bounces it into another electrostatic channel. The second channel decreases the orbit radius slightly so the ions miss the mirror structure even if they gain little energy from the rf. The beam goes through the inner channel and then into the dees for the first time. We expect to get higher transmission through the cyclotron with an external ion source because we will be able to axially focus the beam onto the dee gap. The ions must gain sufficient energy to clear the inner deflector and thereafter the acceleration and extraction and detection proceed as before.

References

(1) K. Nishiizumi and J. R. Arnold, Proc. Symp. on Accelerator Mass Spectrometry, ANL/PHY-81-1 (Argonne, Illinois 1981) p. 262.

(1a) H. Oeschger, talk given at the Symp. on Accelerator Mass Spectrometry (Zurich, Switzerland) 1984

(2) R. A. Muller, Science 196 (1977) 489.

(3) R. A. Muller, P. P. Tans, T. S. Mast, and J. J. Welch, Proc. Symp. on Accelerator Mass Spectrometry, ANL/PHY-81-1 (Argonne, Illinois 1981) p. 342.

(4) J. J. Welch, K. J. Bertsche, P. ?. Freidman, D. E. Morris, R. A. Muller, and P. P. Tans, to be published in Nucl. Instr and Methods

(5) B. R. Doe, report in letter to J. V. Smith, Geochemical Society, June 1983.

(6) W. S. Broecker and T.-H. Peng, Tracors in the Sea, (A publication of the Lamont-Doherty Geological Observatory, Columbia University, Palisades NY, 1982.)

(7) L. A. Currie, talk given at the Symp. on Accelerator Mass Spectrometry, (Zurich, Switzerland) 1984

(8) K. H. Purser, P. Williams, A. E. Litherland, J. D. Stern, H. A. Storms, H. E. Gove, and C. M. Stevens, Nucl. Inst. and Methods 186 (1981) 487.

(9) M. Anbar, Proc. of the 1st Conf. on Radiocarbon Dating with Accelerators, (Rochester, New York) 1978, edited by H. E. Gove.

(10) C. R. Langergren and J. J. Stoffels, Int. J. Mass Spectrom. Ion Phy., 3 (1970) 429

(11) R. Middleton, private communication.

(12) C. D. Jeffries, Phys. Rev. 81 (1951) 1040.

(13) L. G. Smith, Phy. Rev. 111 (1958) 1606.

(14) R. T. McIver Jr., Rev. Sci. Instr. 49(1), (1978) 111.

(15) H. Sommer, H. A. Thomas, and J. A. Hipple, Phys. Rev. 82 (1951) 697.

(16) D. J. Clark, Proc. Tenth Int. Cont. on Cyclotorns and their Applications, (East Lansing, Michigan), (1984)

(17) J. J. Livingood, Principles of Cyclic Particle Accelerators, (D. Van Nostrand Co. Inc., Princeton N. J. 1961).

(18) M. E. Rose, Phys. Rev. 53 (1938) 392.

(19) R. R. Wilson, Phys. Rev. 53 (1938) 408.

(20) P. G. Friedman, (unpublished),

(21) F. Reif, Fundamentals of statistical and thermal physics, (McGraw-Hill, Inc. USA 1965)

(22) H. H. Anderson, private comunication.

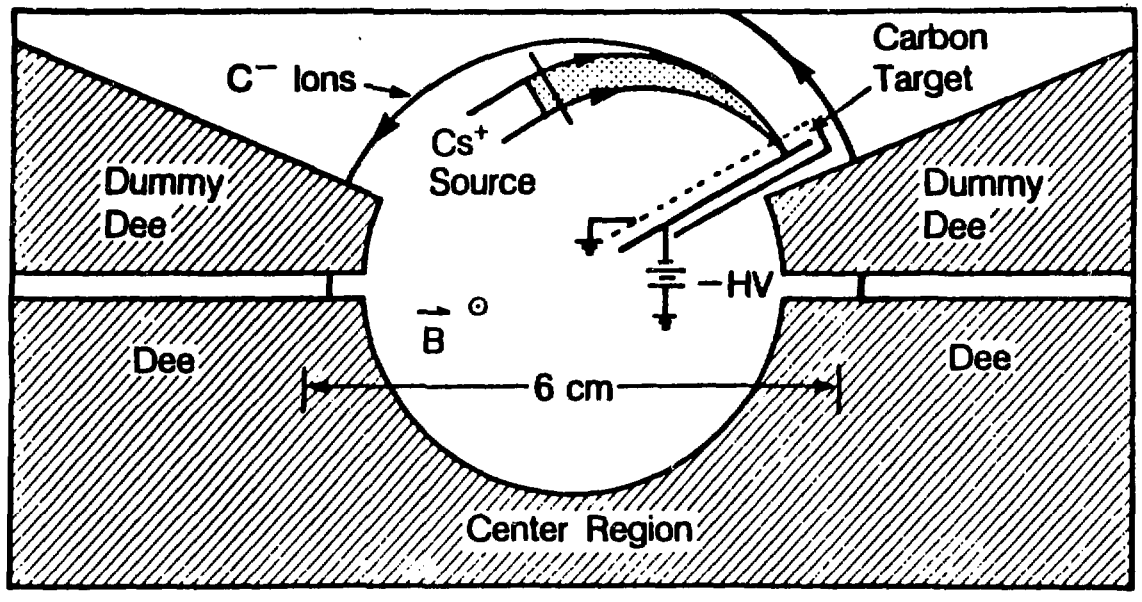

XBL 8410-8758

Figure 1a Positively charged 100 eV cesium ions are focused onto the carbon target biased at -2.8 kV behind a very fine grounded mesh to form negative carbon ions by sputtering. The carbon ions pass by the cesium source structure and, if they have the proper phase, gain energy from the oscillating electric field in the dee - dummy dee gap. The energy gained must be sufficient to enable them to clear the carbon target on the first turn. Subsequent orbits are not shown.

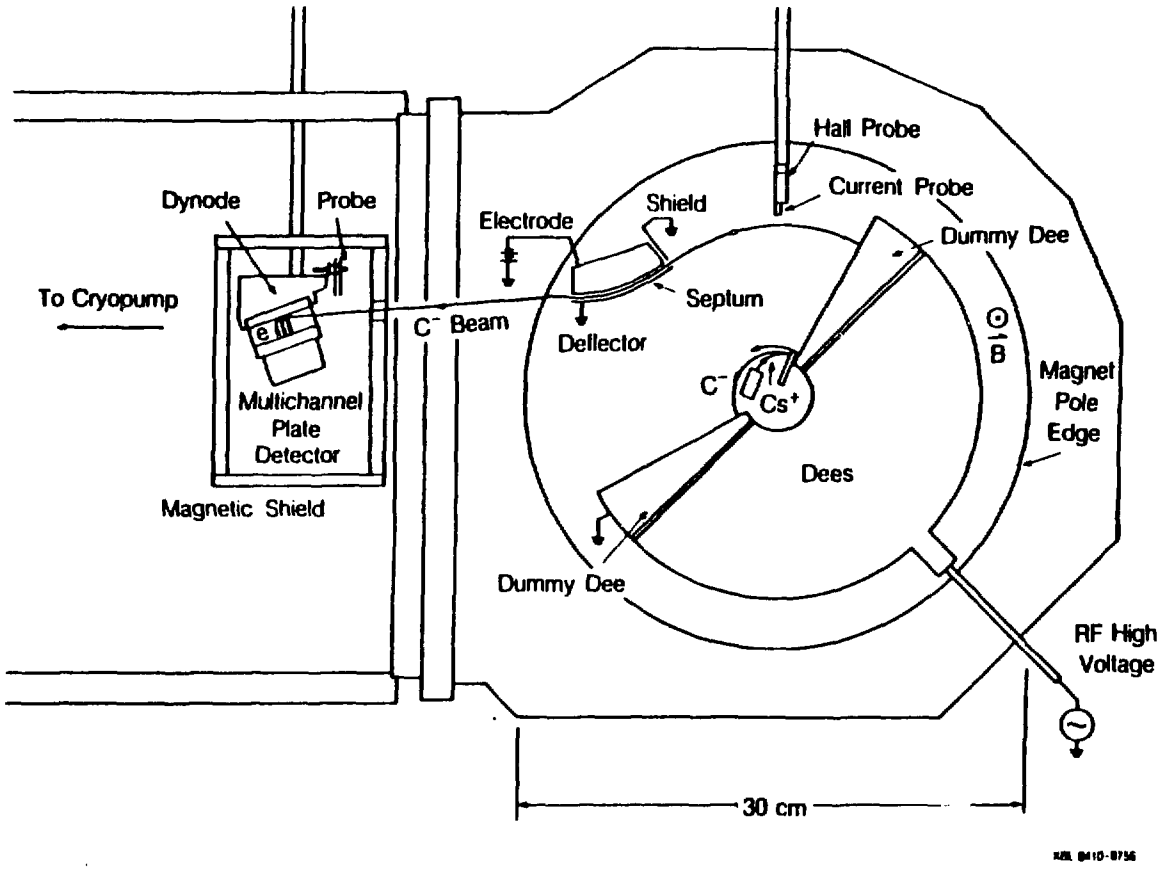

Figure 1b When the carbon ions have reached an energy of 35 keV, their orbit will take them through the thin gap between the grounded septum and an electrode at positive high voltage. The force from the electric field in the gap opposes the magnetic force and deflects the ions out of the magnetic field toward the detector. The detector is located inside a magnetic shield to prevent the fringing field of the magnet pole pieces from affecting the detector. Individual carbon ions can be detected when they strike an aluminum oxide dynode at a glancing angle and emit secondary electrons which are multiplied in a stack of multichannel plates. The operating vacuum is usually about 2×10^{-7} Torr and is provided by a cryopump.

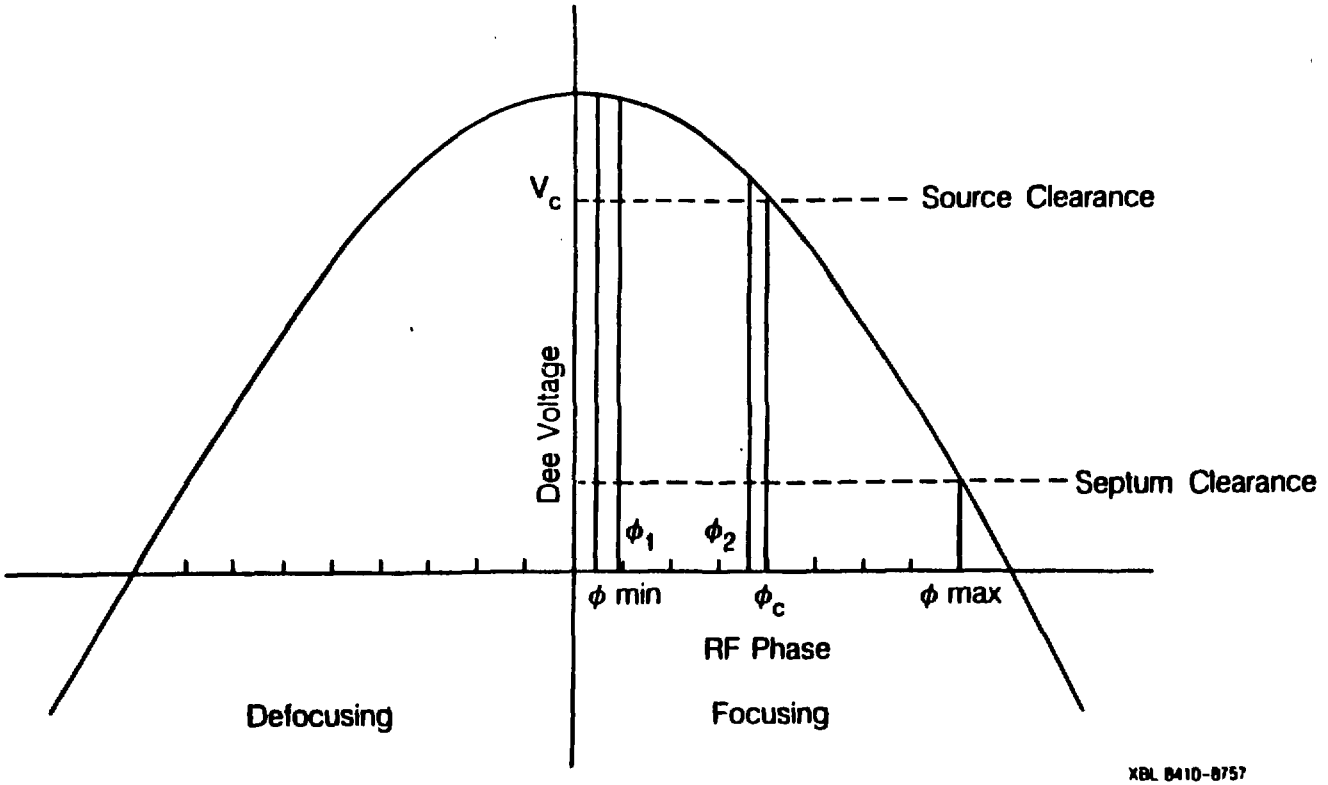

Figure 2 The accelerating rf voltage as a function of phase is shown. The fringing components of the accelerating electric field provide axial focusing for phases between 0 and 180 degrees, but are defocusing from 0 to -180 degrees. ϕ_{max} is the largest relative phase for which ions gain enough energy to clear the septum. ϕ_{min} represents the minimum relative phase for which a significant fraction of the ions can be focused. ϕ_1/ϕ_2 are the minimum/maximum starting phases of a bunch of ions after the first turn. ϕ_c is the largest initial phase which allows ions to clear the source on the first turn.

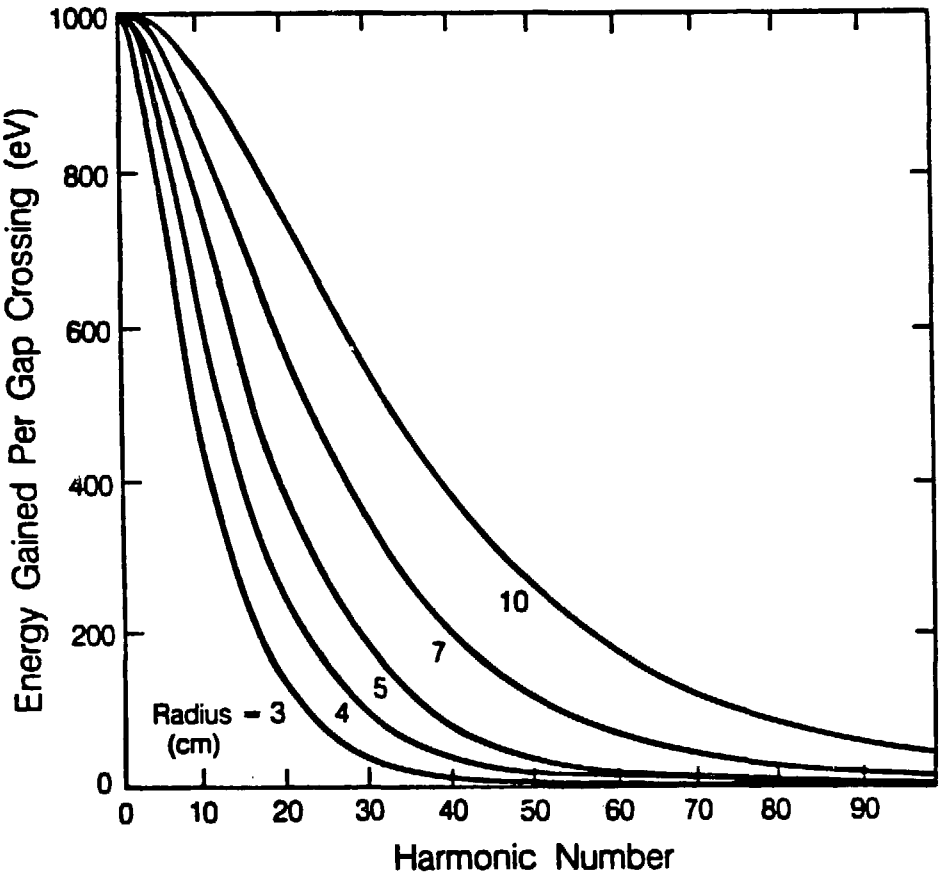

XBL 8410-8759

Figure 3 Shows the calculated energy gained in eV by an ion passing through the accelerating gap exactly in the midplane, versus harmonic number for different radii. The transit time effect almost eliminates energy gain at very high harmonic numbers except when the orbit radii are large. It turns out that for fixed dee geometry, the transit time effect depends only on the ratio of the harmonic number to the radius. Here the distance between the top and bottom dee surface is 8 mm and the rf voltage is 1000 volts 0 to peak.

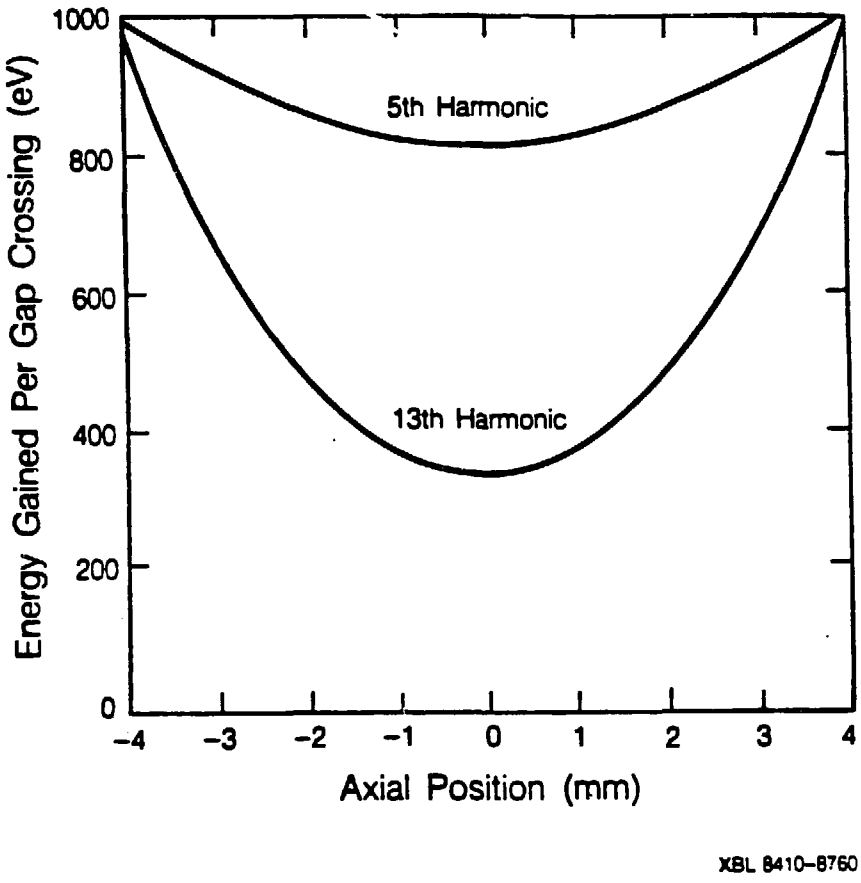

Figure 4 The calculated energy gained by an ion with a 5 cm orbit radius as a function of the distance from the midplane is shown for the 31st harmonic and for the 13th harmonic. The dee voltage is 1000 volts, 0 to peak. The dee surfaces are at 4mm and -4mm. Points within about 1 mm of the dee surface are not representative of real behavior of the low energy cyclotron since the zero gap approximation was used to calculate these curves, and the actual gap is .5mm.

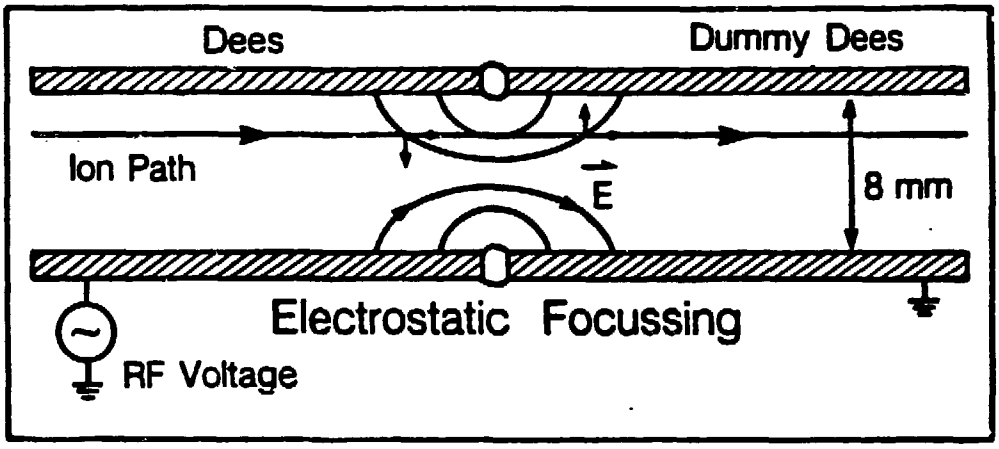

XBL 8410-8761

Figure 5 Electrostatic focusing, also known as phase focusing, is axial focusing which derives from the fringing components of the accelerating electric field. If an ion crosses the gap when the field strength is decreasing the ion is deflected toward the midplane and focused. Defocusing occurs if instead the electric field is increasing.

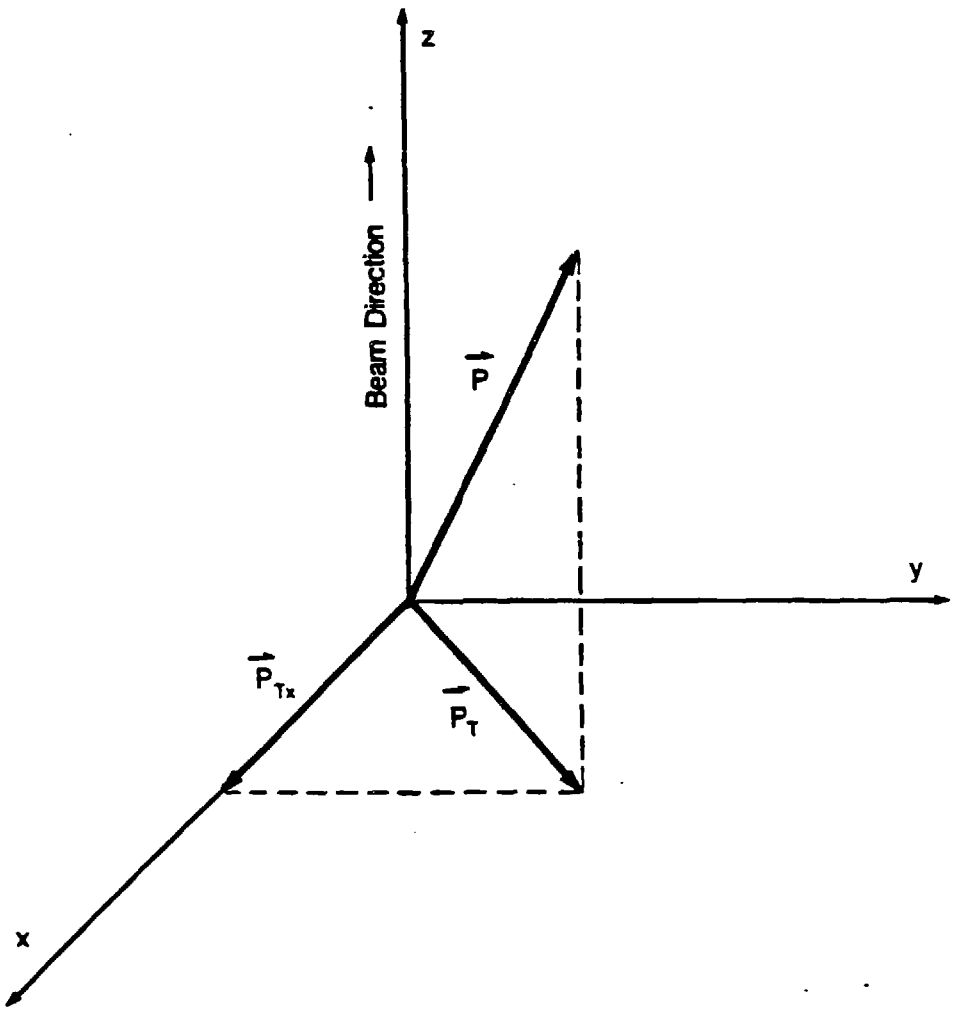

XBL 8410-8762

Figure 6 In general the momentum of a particular ion in the beam will not by exactly along the average direction of the beam. The momentum vector P, is resolved into a component parallel to the beam (along the z direction) and a transverse component, perpendicular to the beam. The transverse component of momentum P_t, may be resolved into a component along an arbitrary direction x which determines the angle of the ion path with respect to the x-z plane and a component perpendicular to the x and z directions.

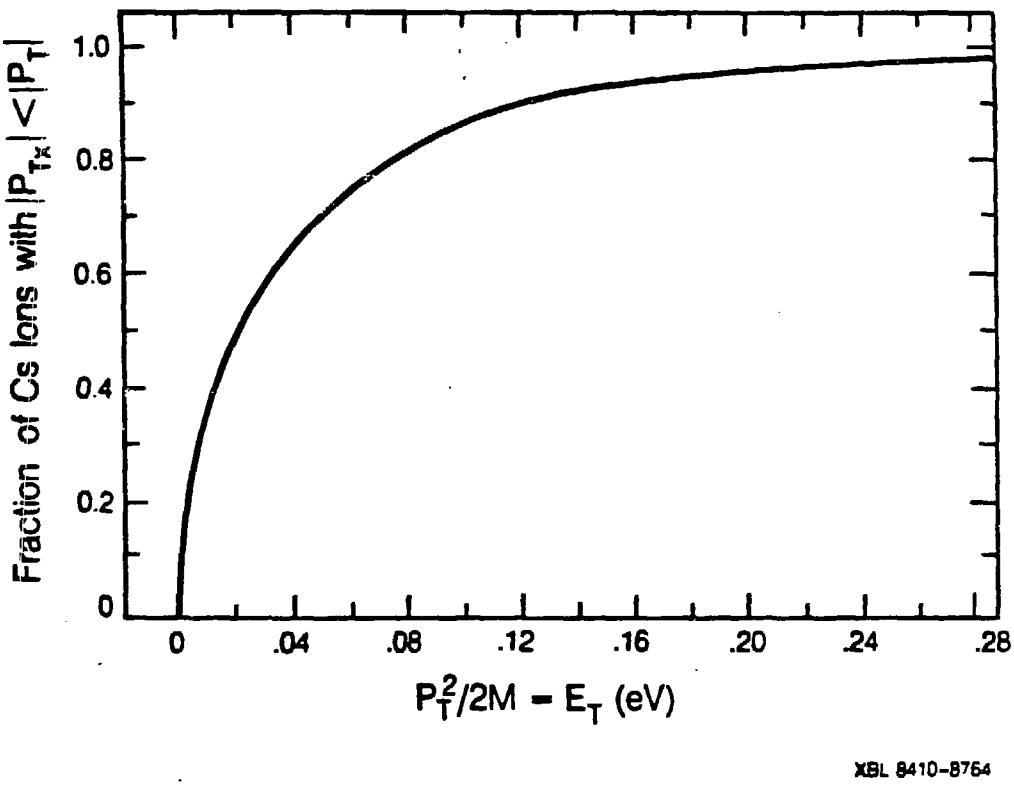

Figure 7a Cesium ions emitted from a hot tungsten surface are distributed in energy and momenta. The calculated fraction of cesium ions whose component of momentum in the radial direction is less than an arbitrary P_t, is plotted against E_t, where $E_t = /P_t/^2 /2M$. This plot can be used to determine the fraction of ions whose paths are contained within a given radial angle.

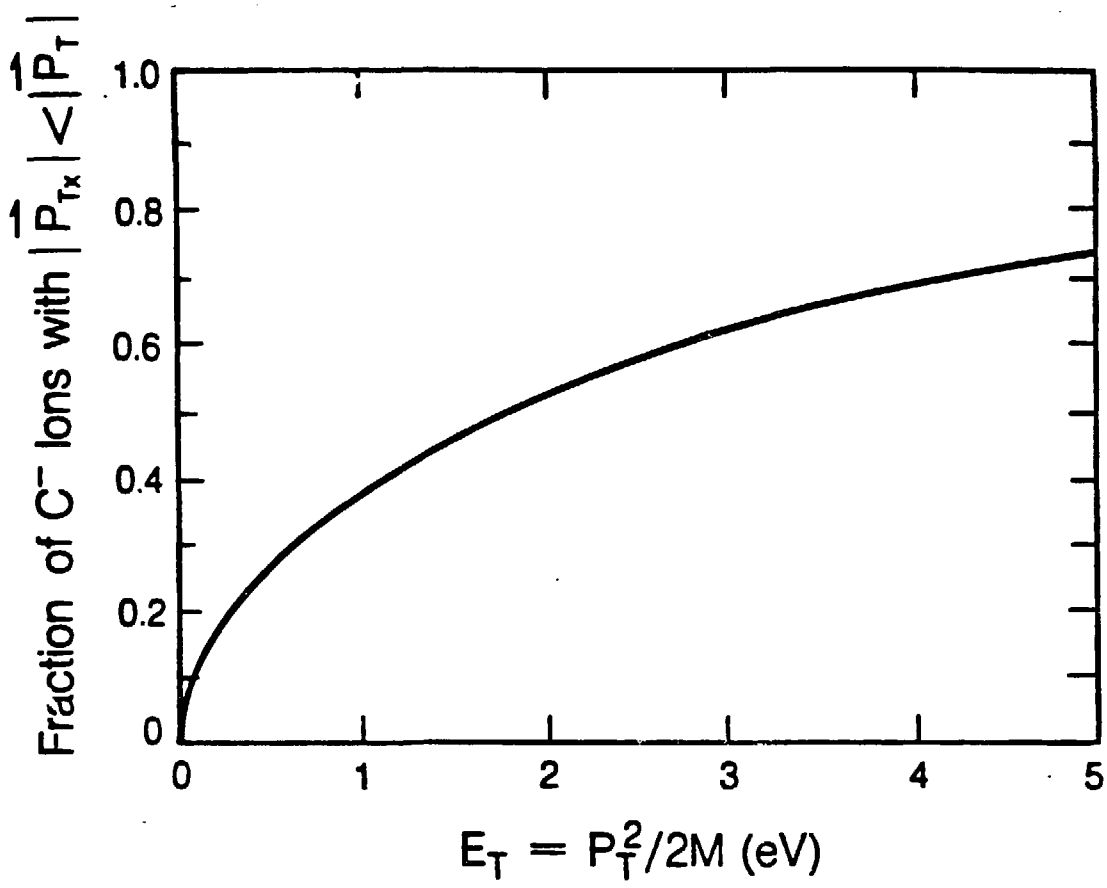

XBL 8410-8763

Figure 7b Carbon ions which are sputtered from a carbon surface by cesium ions, are distributed in energy and momenta according to the kinetics of the sputtering process. The calculated fraction of the carbon ions whose component of momentum in the radial direction is less than an arbitrary P_t is plotted against E_t, where $E_t = /P_t/^2/2M$.

Figure 7b

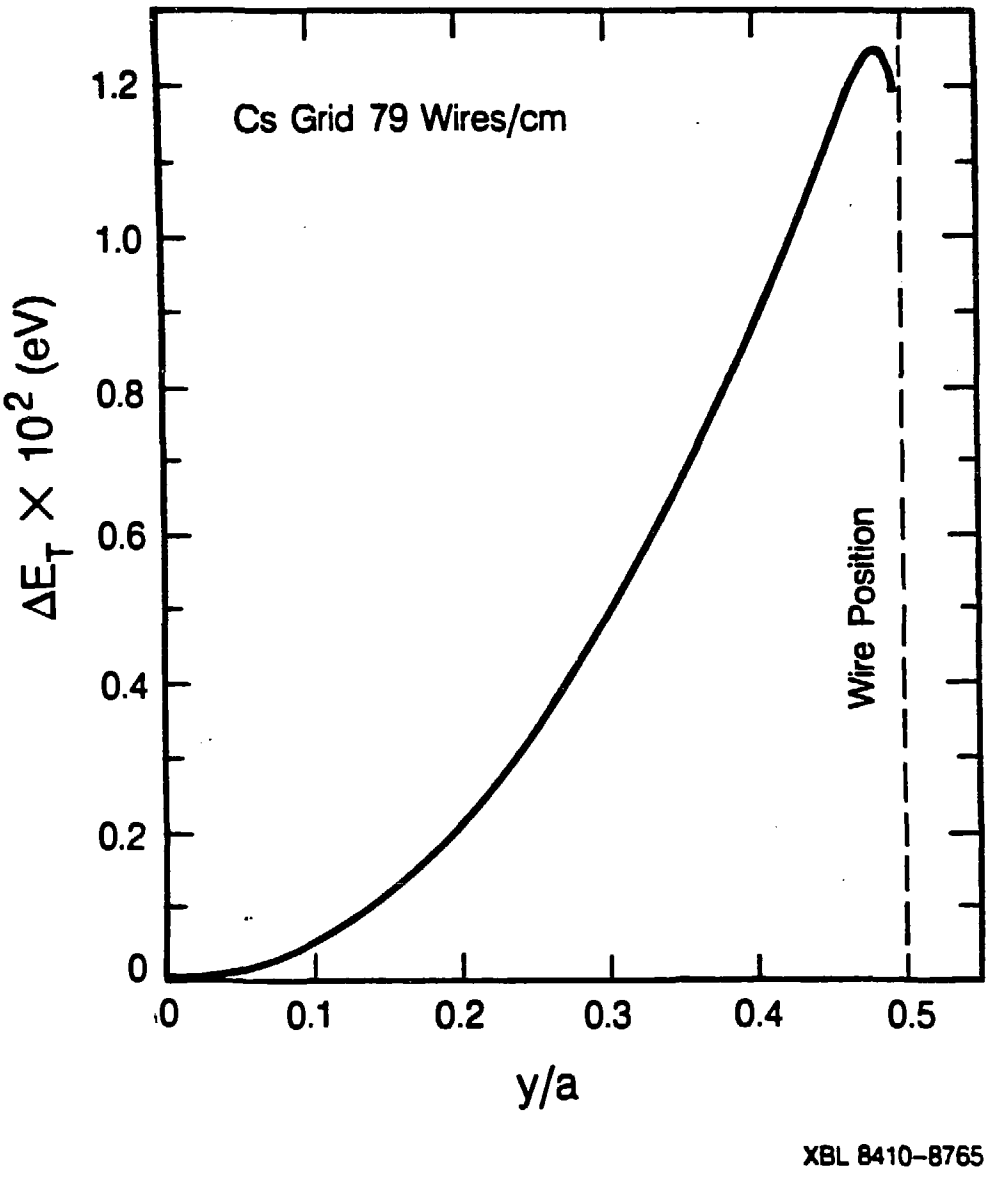

Figure 8a The increase in transverse energy of a cesium ion due to passage through the field defining rectangular mesh is shown. The distance between wires on the mesh is a and the distance from the center of the mesh rectangle to the ion path is y.

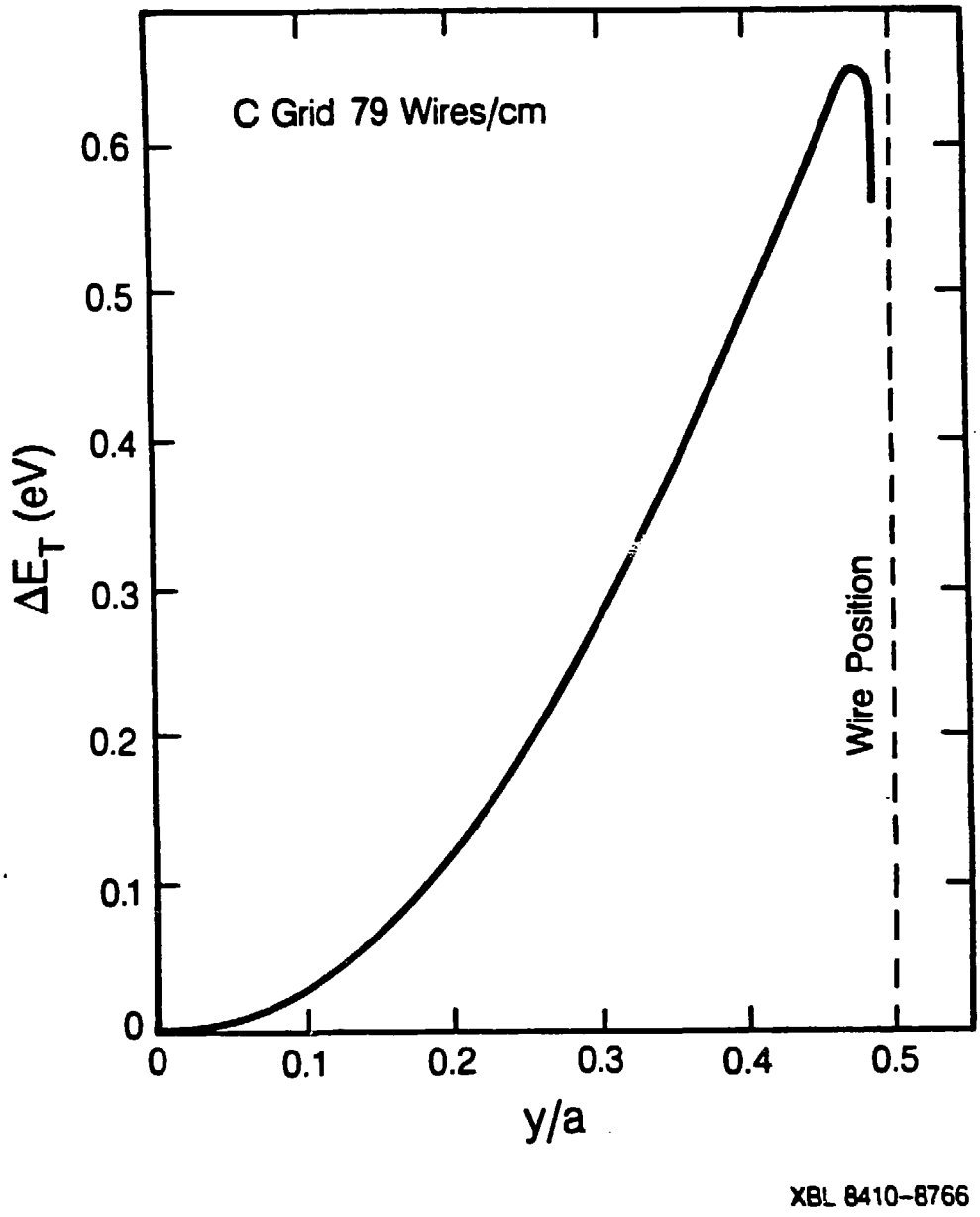

Figure 8b The increase in transverse energy of a carbon ion due to passage through the field defining rectangular mesh is shown. The distance between wires on the mesh is a and the distance from the center of each mesh rectangle to the ion path is y.

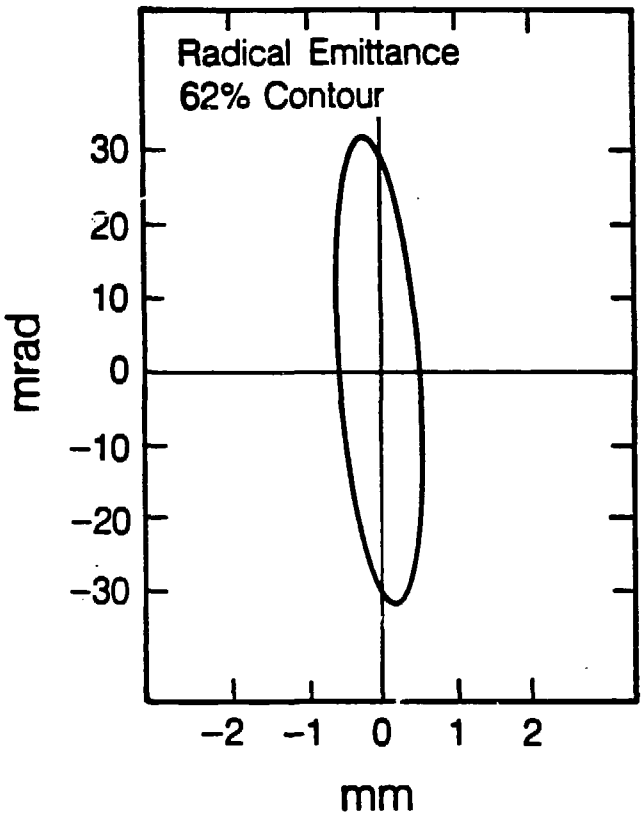

XBL 8410-8768

Figure 9a This plot shows the 62% contour of the radial emittance of the carbon ions. This was calculated for 2700eV ions at the point where they enter the accelerating gap for the first time.

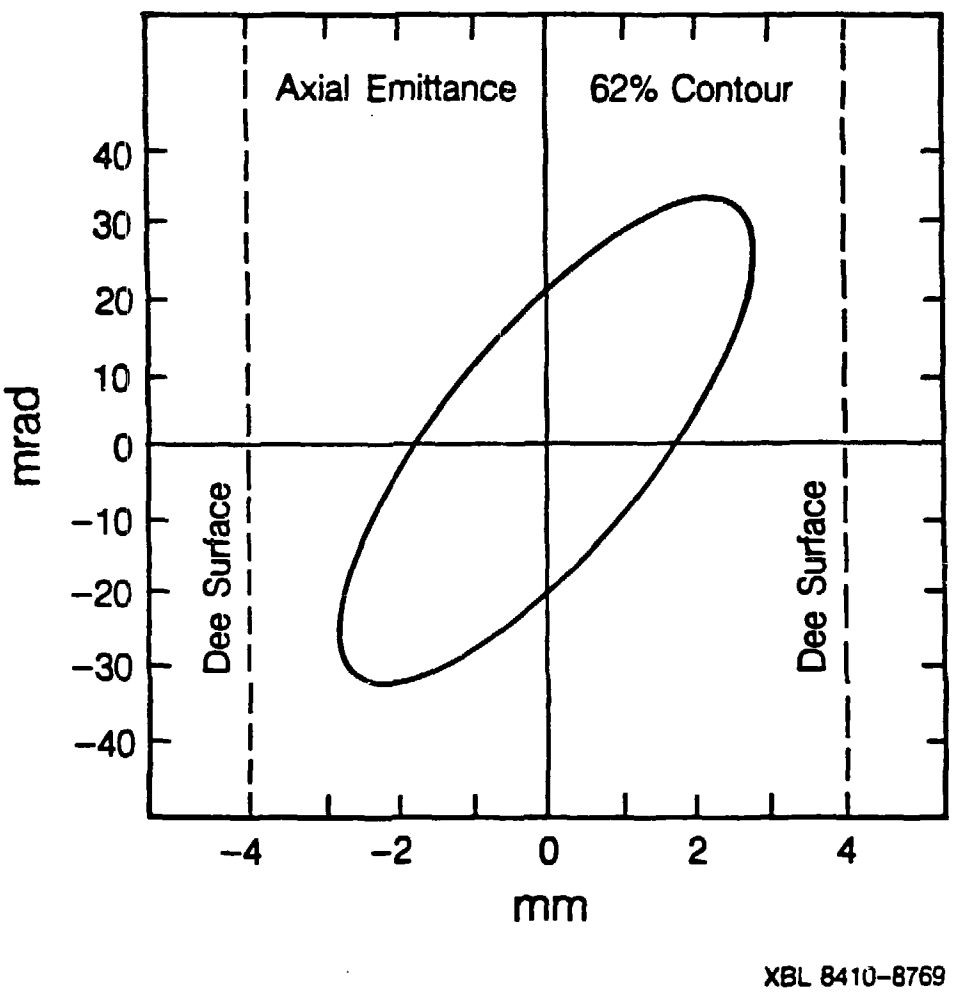

Figure 9b The axial emittance was calculated for the carbon ions when they enter the accelerating gap for the first time and are axially focused. The 62% contour is shown and the energy of the ions is 2700 eV.

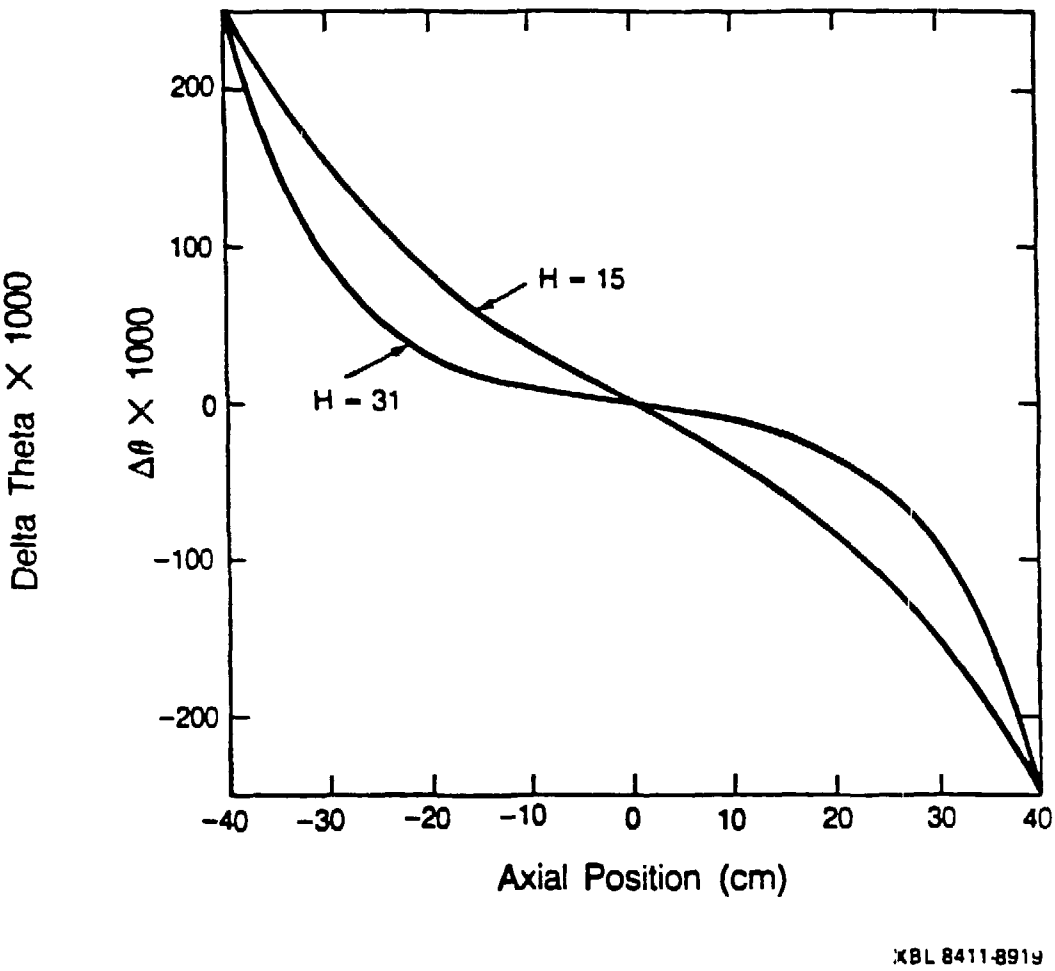

Figure 10 The angle by which an ion traveling perpendicularly to the accelerating gap is deflected by the electric field in the gap is shown versus the distance from the midplane for two different harmonic numbers. Low harmonics give thin lens like behavior where the angle is proportional to the distance from the midplane, while for high harmonics the behavior is distinctly non linear. The radius was 3 cm and the dee voltage was 1000 volts (0 to peak) at 30 degrees of rf phase.

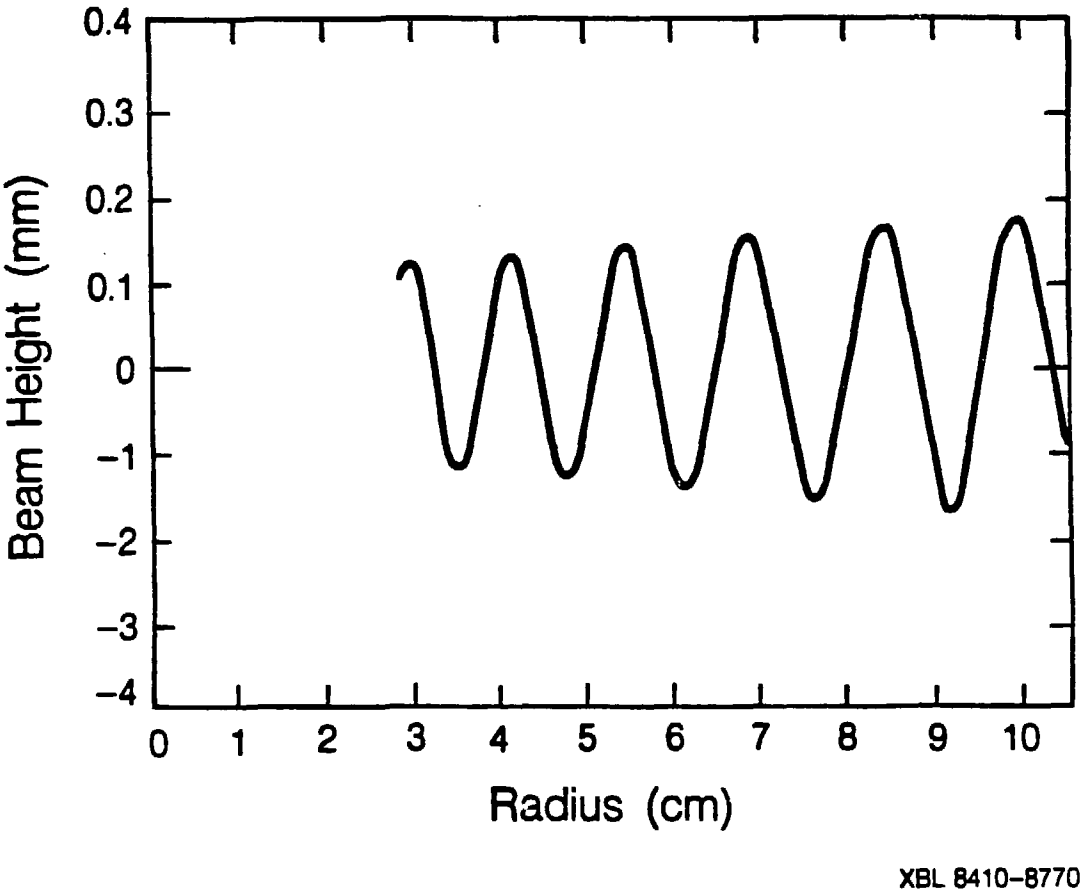

Figure 11a The calculated axial position of a ^{14}C ion as a function of radius is shown for a typical ion on the 13th harmonic with 1300 volts (peak to peak) on the dees. This ion starts 1 mm off the midplane with a transverse energy of .27 eV, and accelerates at a constant of 30 degrees of rf phase to the final energy of 36 keV in 40 turns.

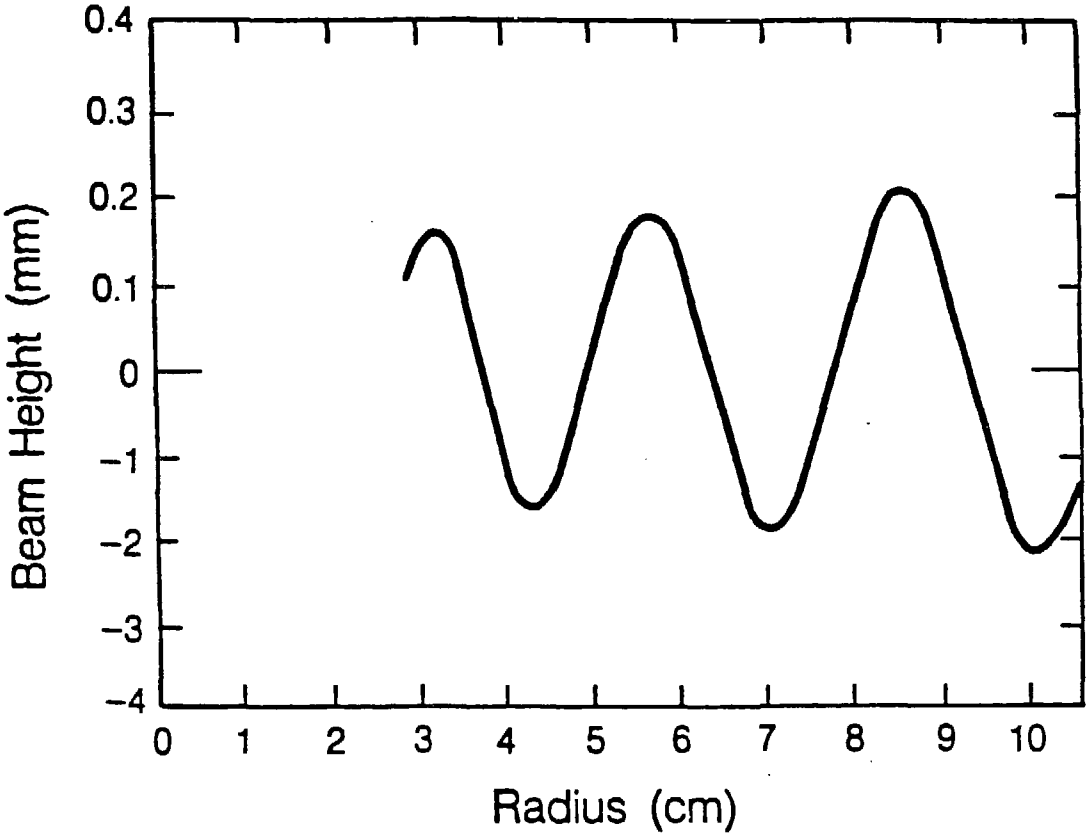

XBL 8410-8772

Figure [illegible] This ion has the same parameters as in 11a except the phase angle has been reduced to 10 degrees. This results in weaker focusing and fewer axial oscillations. V_z is only .08 compared to V_z of .14 at 30 degrees phase.

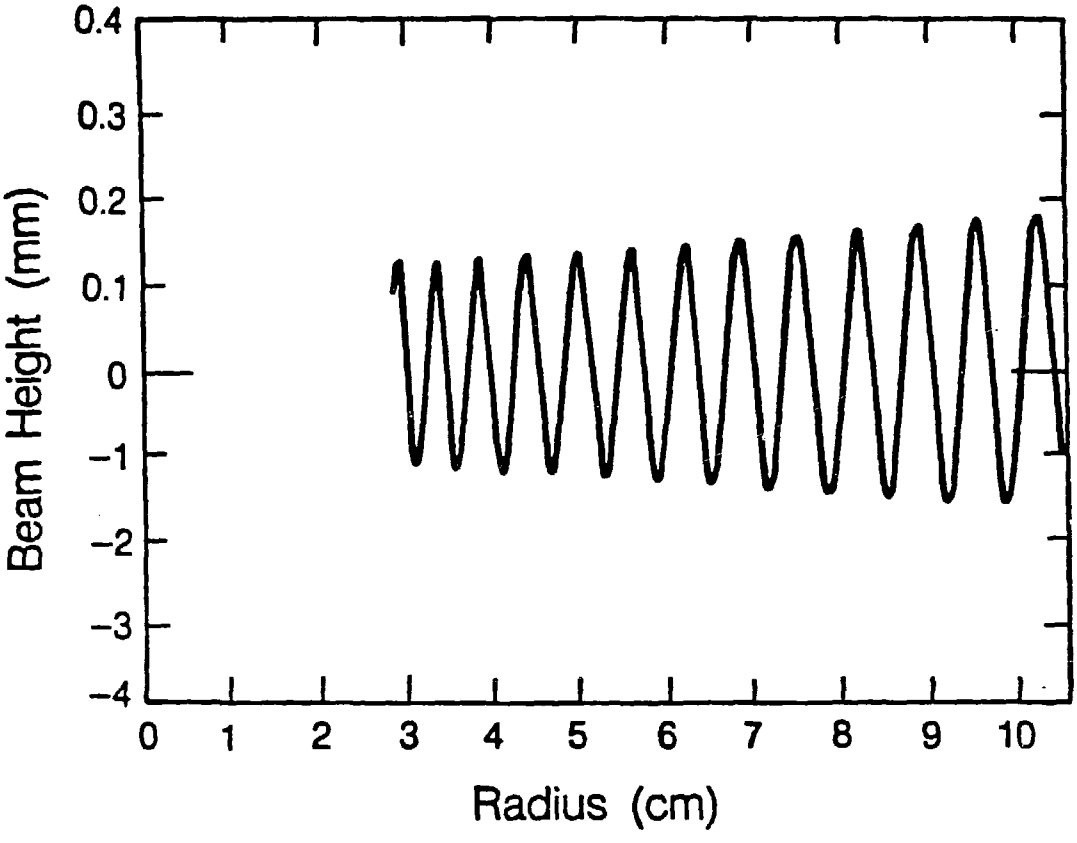

Figure 11c This plot shows the axial motion of ion with the same parameters as in 11a but an rf phase of 60 degrees. Larger phase gives stronger focusing, (V_z is .18), but less energy gain per turn. This ion took 69 turns to reach the full energy.

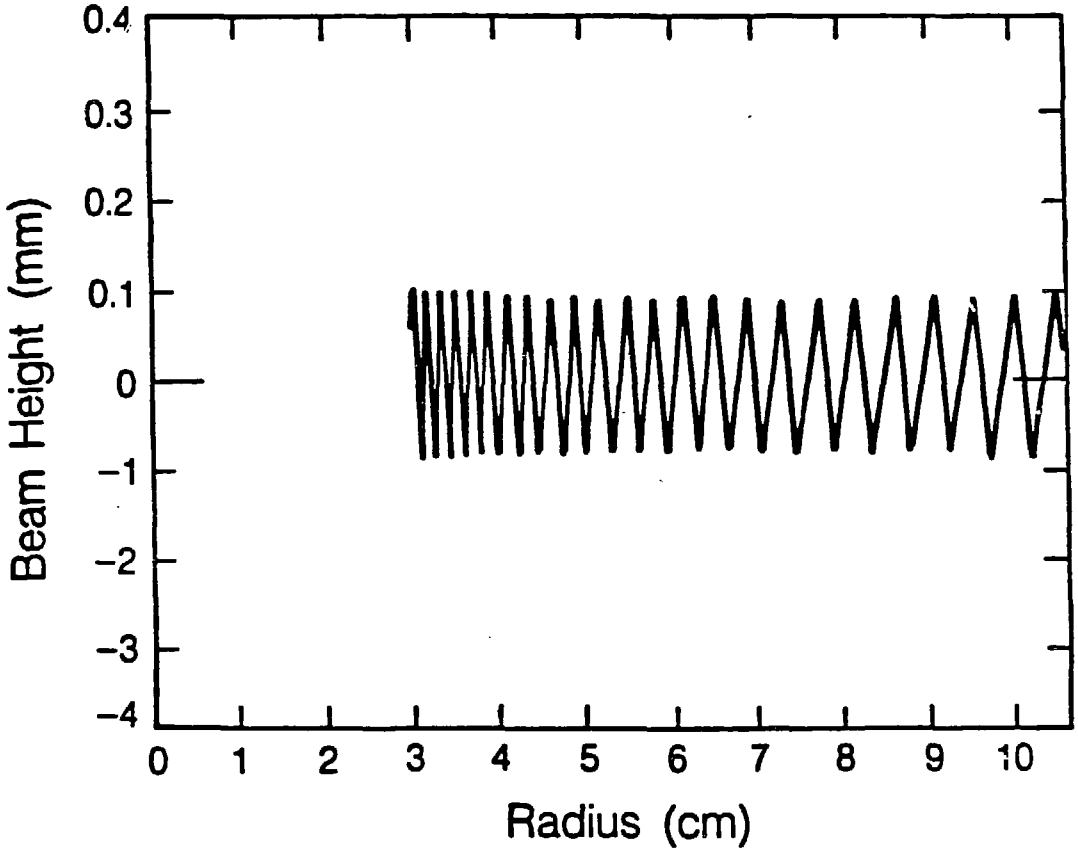

Figure 11d This trajectory shows a decrease in the amplitude of oscillation until about 5 cm radius and then a gradual increase in amplitude. This is obtained by operating at the 31st harmonic with a ^{14}C ion which started 0.5mm above the midplane with a transverse energy of 0.1 eV at 45 degrees of rf phase. The dee voltage has been turned down to 1000 volts peak to peak and the ion took 181 turns to reach the full energy. V_z is 0.13.

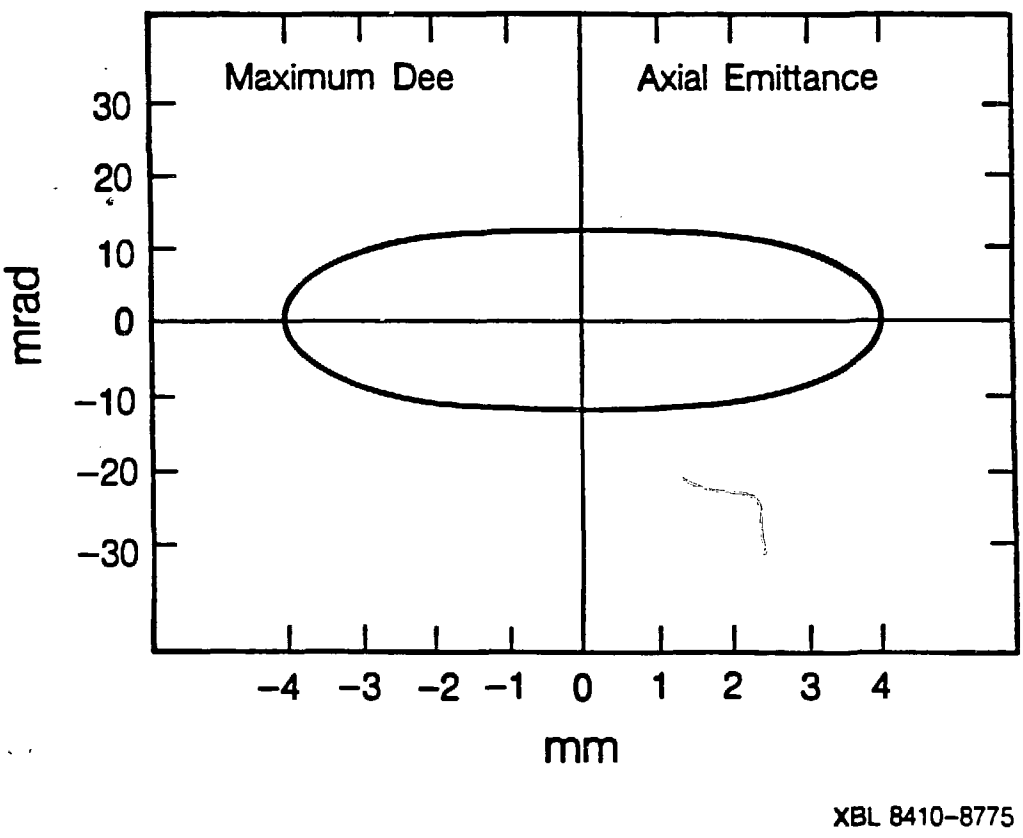

Figure 12 The calculated maximum dee emittance is shown in figure 12. The contour should contain all possible orbits, as calculated by the orbit simulation program, which start at 3 cm with the 13th harmonic and 1300 volts peak to peak dee voltage.

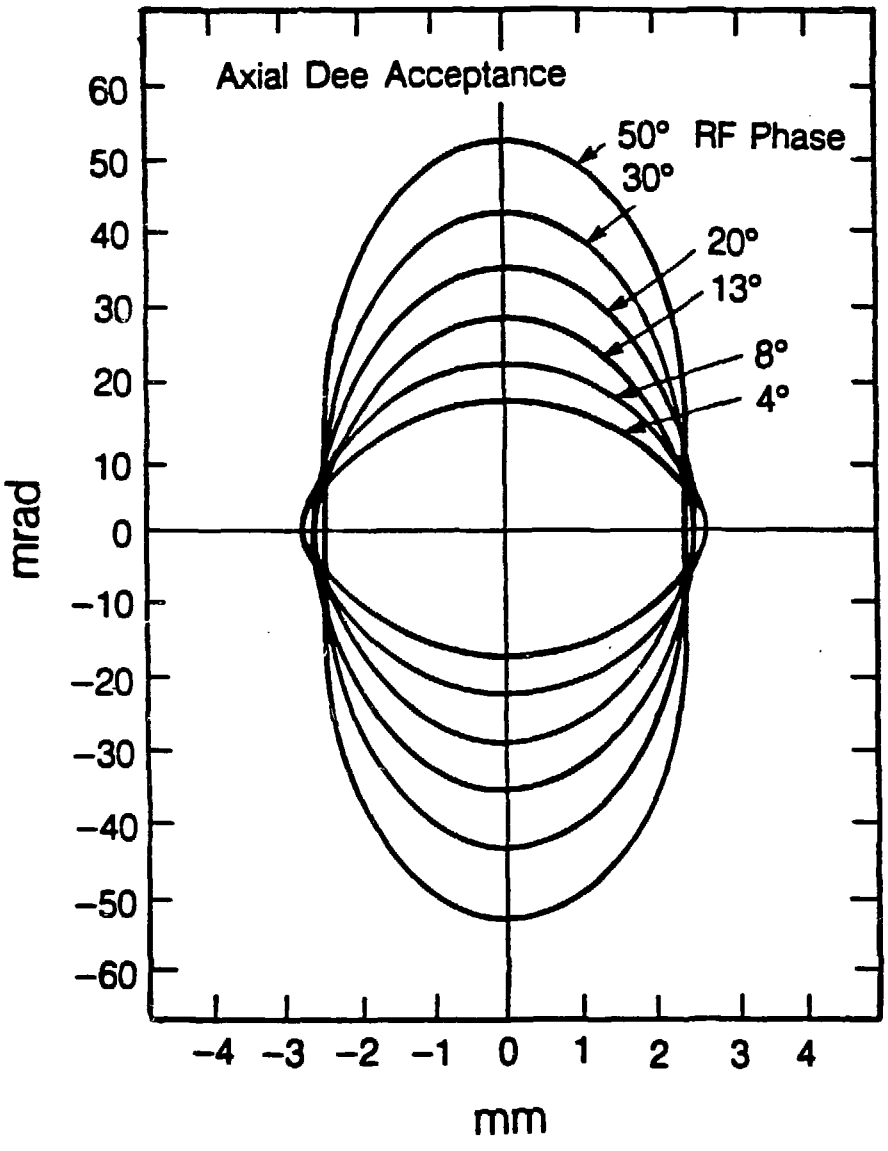

XBL 8410-8774

Figure 13 This plot shows the acceptance of the cyclotron from the ion source to the extraction radius for various rf phases, determined from the orbit simulation program. Note that the acceptance does not match well with the axial emittance shown in figure 9b as many ions are too far from thr midplane to be contained within the dees, and accounts for some of the initial current loss.

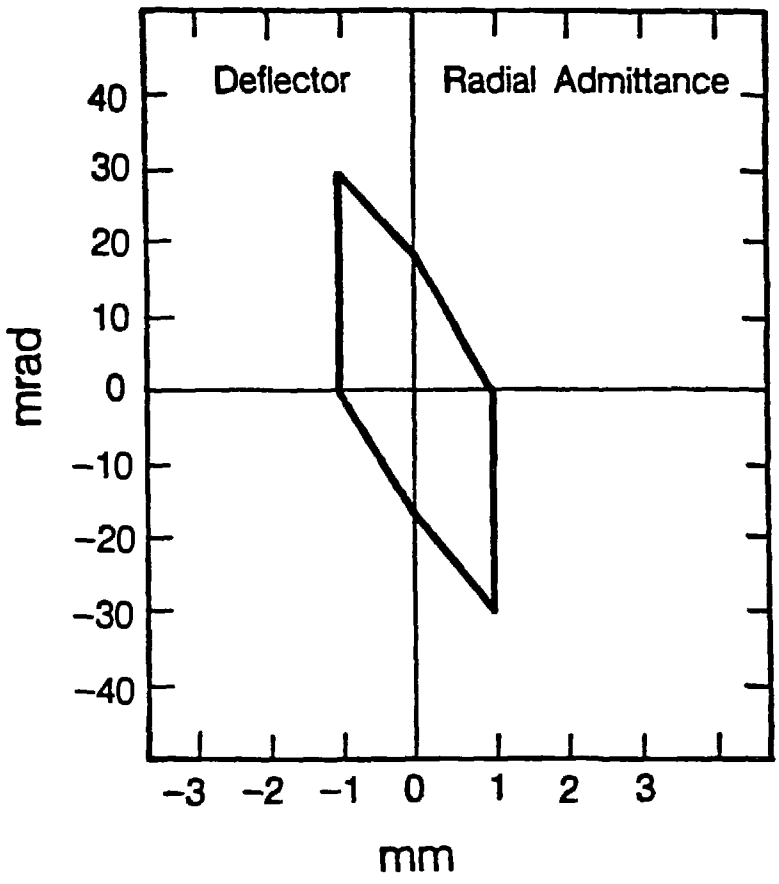

Figure 14 The deflector radial admittance is shown in this figure. It was calculated for monoenergetic ions and only includes ions which have cleared the septum and entered the 2 mm gap between the septum and the positive electrode.

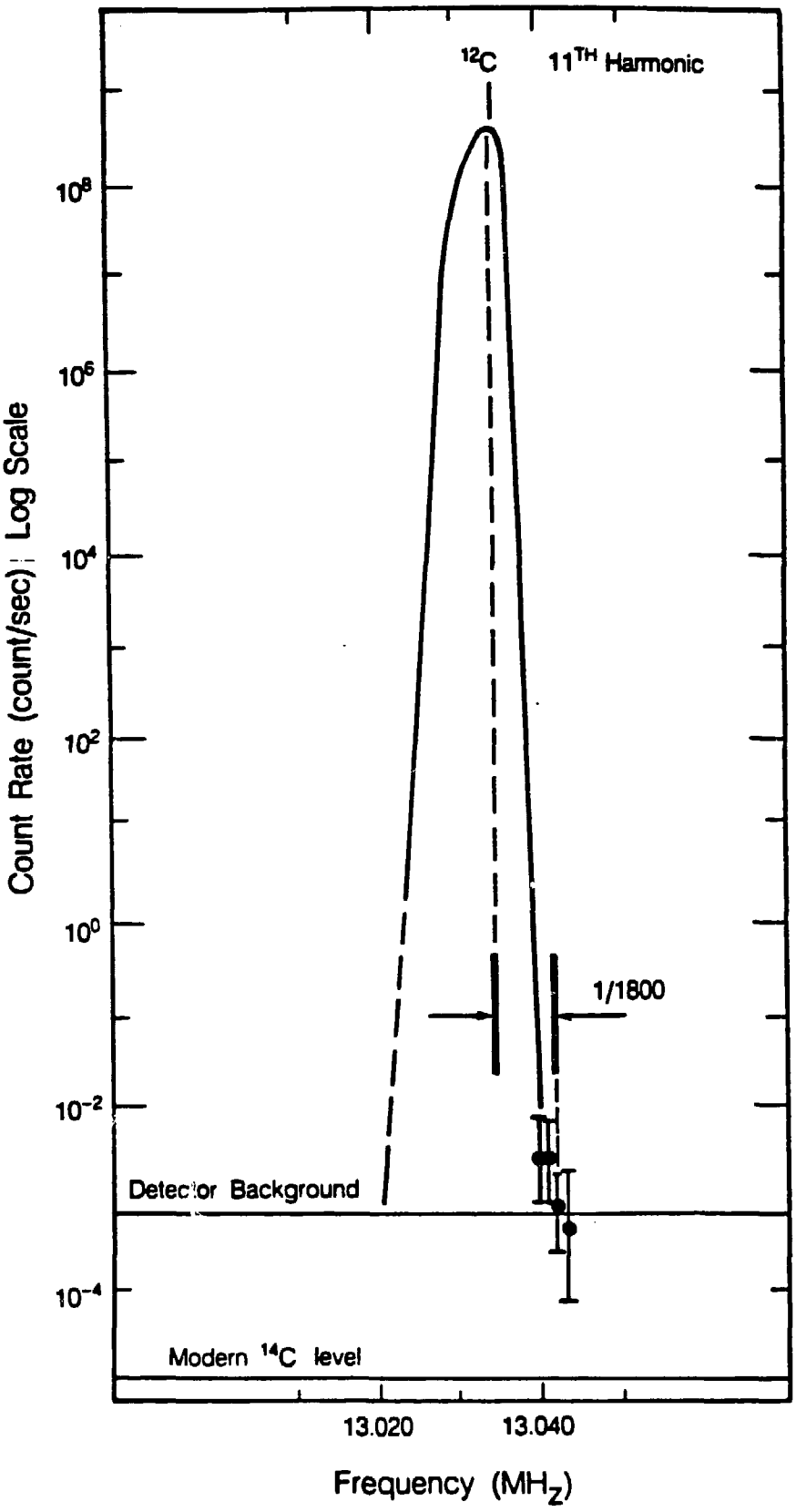

Figure 15

XBL 8410-8777

Figure 15 The cyclotron was tuned to accelerate a strong ^{12}C beam on the 11th harmonic and the count rate versus rf frequency is shown in this figure. The ^{12}C peak is rejected by a factor of 2×10^{-11} at 1/1800 separation in frequency, (equivalent to a mass separation of 1/1800). The detector background (1 count in 20 minutes) and the limited ion source current prevented measurement of the tails of this peak below this level. The height of the peak was determined independently by a faraday cup in place of the detector, and by detector measurements of the tail which showed how much the current increased as the source power was turned up. The shape of the top part of the peak, where the count rate exceeded the detectors limit of about 3×10^4 counts per sec, was extrapolated from low current measurements and was found not to vary significantly over many orders of magnitude. Based on the height of the peak, one would expect to see a count rate from samples with modern ^{14}C concentrations about a factor of 50 below the detector background. Where error bars are not shown they are about 10% of the rate or less.

Figure 16 The tuning curve near the ^{14}C reasonance at the 13th harmonic shows no background of ^{14}C and more than adequate mass resolution to eliminate the interference due to $^{13}CH^-$. During this measurement, the source current was about what was used to obtain the tuning curve in figure 15. Error bars pointing downward indicate the 84% confidence interval for 0 counts during the measurement period.

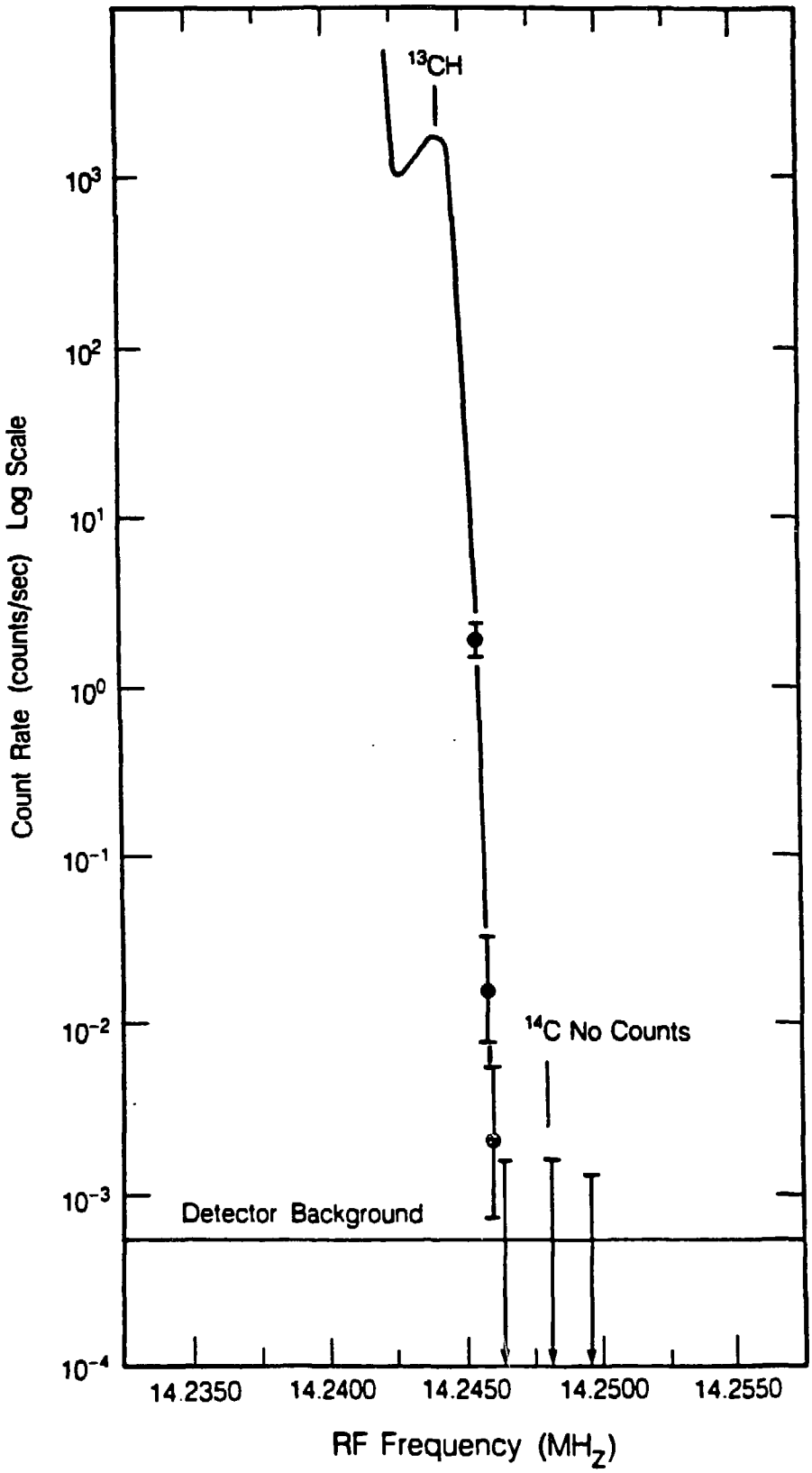

Figure 16

XBL 8410-8776

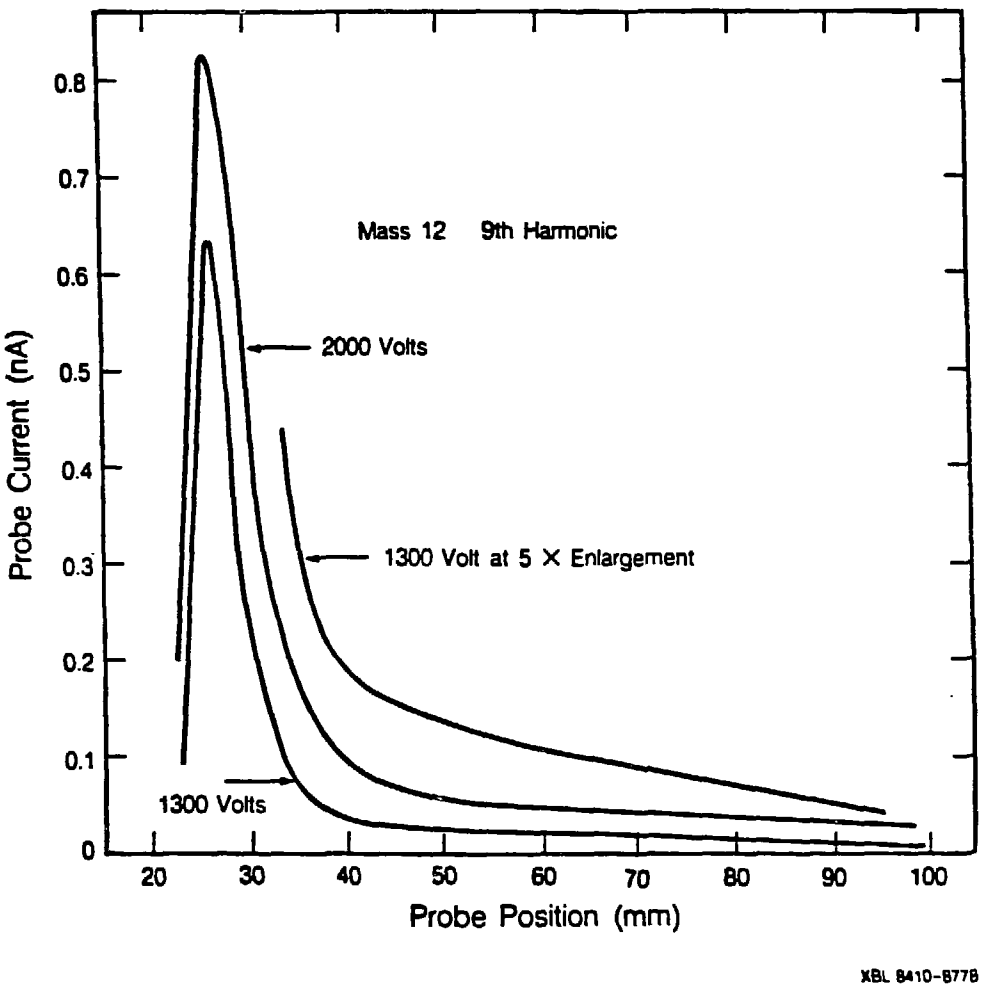

Figure 17 The current intercepted by a movable probe is plotted against radial position for mass 12 on the 9th harmonic. Most of the current loss occurs within the first quarter of the orbits. At high rf voltage, (2000 volts peak to peak), the transmission is better due to the stronger focusing.

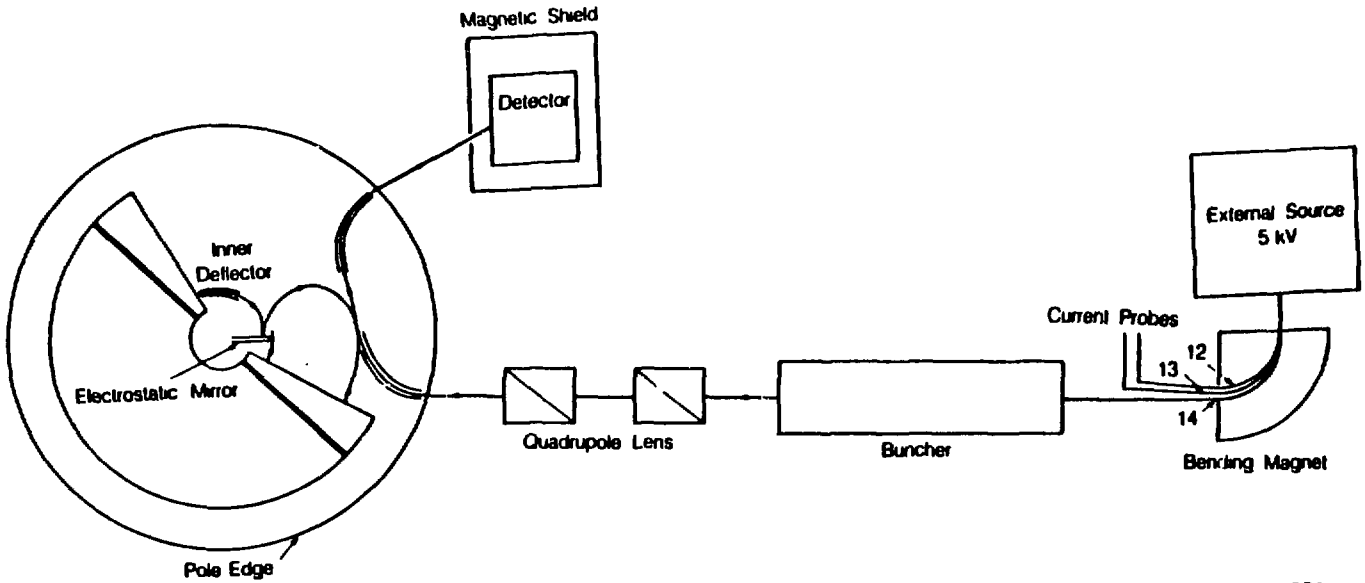

Figure 18 The scheme for radially injecting ions from an external ion source into the center of the cyclotron is shown in this figure. The beam from a conventional negative carbon ion source is sent through a bending magnet where the mass 12 and 13 beams are removed and measured. A buncher velocity modulates the beam so that the ions bunch at the first gap crossing. A deflector beings the beam into the magnet and directs it to an electrostatic mirror which bounces it through another deflecting channel and then into the dees where acceleration, focusing and extraction proceed as before. The bending magnet may be replaced by an ExB velocity selector which has the advantage of eliminating high velocity mass 12 and 13 ions which will be present in sputter ion source.

Table of Contents